

NASA Technical Memorandum 100695

(NASA-TM-100695) VERIFICATION OF REGIONAL
CLIMATES OF GISS GCM. PART 1: WINTER (NASA)
51 p CSCL 04B

N88-26012

Unclas

G3/47 0149513

VERIFICATION OF REGIONAL CLIMATES OF GISS GCM- Part 1 : Winter

LEONARD M. DRUYAN
and
DAVID RIND

January 1988



National Aeronautics and
Space Administration

Goddard Institute for Space Studies
Goddard Space Flight Center

NASA Technical Memorandum 100695

**VERIFICATION OF REGIONAL CLIMATES
OF GISS GCM- Part 1 : Winter**

**LEONARD M. DRUYAN
and
DAVID RIND**

January 1988



**National Aeronautics and
Space Administration**

**Goddard Institute for Space Studies
Goddard Space Flight Center**

Foreword

The GCM used for climate studies at GISS is now second generation (model II). It was described in the Monthly Weather Review in 1983 in a 53-page article by Hansen, Russell, Rind, Stone, Lacis, Lebedeff, Ruedy and Travis. This benchmark publication discussed the computational schemes as well as the research that created model II from its predecessor and characteristics of the model climate. Regional details of the simulated climate for fine and medium resolutions ($4^{\circ}\text{lat} \times 5^{\circ}\text{long}$ and $8^{\circ}\text{lat} \times 10^{\circ}\text{long}$) were beyond its scope.

Since models computed at grid resolutions no finer than $4^{\circ} \times 5^{\circ}$ do not resolve many synoptic weather features very well, one must be cautious about interpreting their results for specific geographic locations. Time and space averaging of model output can certainly make it more meaningful. Still, a seemingly successful verification of zonal mean fields may mask very serious deficiencies, such as when errors of opposite sign cancel each other. When the errors derive from computational instabilities or small displacements of features (that may result from the limitations of the spatial resolution), then the smoothing accomplished by zonal averaging is desirable. When, however, the errors derive from a poor simulation of the characteristics of major circulation features, then the emphasis on accurate profiles of a zonal mean quantity is misleading. (Consider, for example, that if a maritime high and a continental low at the same latitude were both simulated to be too shallow, it would not show up in the zonal mean of the sea-level pressure.) Moreover, one cannot ignore the components of monsoonal circulations in favor of tropical or subtropical zonal means, nor should one overlook the blurring of southwestern deserts with southeastern humid zones because the zonal mean precipitation rate verifies well. Naturally, verifiable model success in depicting regional climates generates confidence that the larger-scale features are realistic for the right reasons.

A number of interesting and useful model applications relate to regional climates and they require a complete understanding of the unperturbed models' faithfulness to the actual climate of the zone under study. A model prediction of the double-CO₂ climate of Europe is more believable when the model has been shown to simulate today's European climate realistically.

Sea-level pressure fields and precipitation rates are compared to analyses of observed data published by Dennis Shea in his Climatological Atlas (NCAR, 1986). The data cover the years 1950-79.

The components of the wind aloft and the surface wind are verified against analyses by Abraham Oort in his Global Atmospheric Circulation Statistics (NOAA, 1983). These data cover the period 1963-1973. Qualitative comparison of surface flow is made with analyses of the gradient wind by Atkinson and Sadler (US Air Force, 1970) and a streamflow analysis over North America made by NAVAIR (1966) but published by Bryson and Hare in their Climates of North America (Elsevier, 1974).

Two versions of model II have been chosen for the present verification study. The fine grid, for which computations are made at a horizontal resolution of 4° latitude by 5° longitude, was run for five consecutive model years as 848F9. It used prescribed, climatological sea-surface temperatures, time-interpolated to each day of the year. The discussion in this presentation relates to the mean fields for the five years.

The medium grid version is computed at the spatial resolution of 8° latitude by 10° longitude. It was run for 37 model years as 882M9, but the fields shown in this presentation represent the means for the ten model years 26-35. This version computes the sea-surface temperature as a by-product of the air/sea energy exchange based on prescribed, seasonally varying values of heat transport within the ocean. Mean monthly and seasonal sea-surface temperatures generated by this interactive ocean formulation have been shown to be climatologically realistic.

Part I, Winter: December-January-February means

1. Verification of fine and medium grid sea-level pressures (SLP) and precipitation rates for North America, Pacific and Atlantic Oceans (Northwest Quarter).....	1
2. Verification of fine and medium grid SLP and precipitation rates for the Eastern Hemisphere.....	6
3. Verification of fine and medium grid SLP and precipitation rates for South America, tropical and South Pacific Ocean (Southwest Quarter).....	13
4. Verification of fine and medium grid 7th-layer (200mb) zonal wind, Northwest Quarter.....	17
5. Verification of fine and medium grid 7th-layer (200mb) zonal wind, Eastern Hemisphere.....	20
6. Comparison of models' resultant surface winds to streamflow analyses based on observed gradient and surface winds.....	23
7. Verification of fine and medium grid surface zonal wind, Northwest Quarter.....	23
8. Verification of fine and medium grid surface zonal wind, Eastern Hemisphere.....	28
9. Verification of fine and medium grid surface meridional wind, Northwest Quarter.....	31
10. Verification of fine and medium grid surface meridional wind, Eastern Hemisphere.....	34
11. Cross-equatorial flow.....	36

List of Figures	Page
1.1 SLP, fine grid, Northwest Quarter.....	4
1.2 SLP, observed, Northwest Quarter.....	4
1.3 SLP, medium grid, Northwest Quarter.....	4
1.4 Precipitation rates, fine grid, Northwest Quarter.....	5
1.5a Precipitation rates, observed, Northwest Quarter.....	5
1.5b Precipitation rate errors, fine grid-observed, NW Quarter.....	5
1.6 Precipitation rates, medium grid, Northwest Quarter.....	5
2.1 SLP, fine grid, Europe and Africa.....	9
2.2 SLP, observed, Europe and Africa.....	9
2.3 SLP, medium grid, Europe and Africa.....	9
2.4 Precipitation rates, fine grid, Europe and Africa.....	10
2.5a Precipitation rates, observed, Europe and Africa.....	10
2.5b Precipitation rate errors, fine grid-observed, Europe & Africa..	10
2.6 Precipitation rates, medium grid, Europe and Africa.....	10
2.7 SLP, fine grid, Asia and Indian Ocean.....	11
2.8 SLP, observed, Asia and Indian Ocean.....	11
2.9 SLP, medium grid, Asia and Indian Ocean.....	11

2.10	Precipitation rates, fine grid, Asia and Indian Ocean.....	12
2.11a	Precipitation rates, observed, Asia and Indian Ocean.....	12
2.11b	Precipitation rate errors, fine grid-observed, Asia & Indian O.	12
2.12	Precipitation rates, medium grid, Asia and Indian Ocean.....	12
3.1	SLP, fine grid, South America and South Pacific Ocean.....	15
3.2	SLP, observed, South America and South Pacific Ocean.....	15
3.3	SLP, medium grid, South America and South Pacific Ocean.....	15
3.4	Precipitation rates, fine grid, South America and S. Pacific O...	16
3.5a	Precipitation rates, observed, South America and S. Pacific O...	16
3.5b	Precipitation rate errors, fine grid-observed, S. Amer./S. Pac..	16
3.6	Precipitation rates, medium grid, South America and S. Pacific...	16
4.1	U-component of 7th-layer wind (200mb), fine grid, NW Quarter.....	19
4.2	U-component of 200mb wind, observed, Northwest Quarter.....	19
4.3	U-component of 7th-layer wind, medium grid, Northwest Quarter....	19
5.1	U-component of 7th-layer wind, fine grid, Eastern Hemisphere.....	22
5.2	U-component of 200mb wind, observed, Eastern Hemisphere.....	22
5.3	U-component of 7th-layer wind, medium grid, Eastern Hemisphere...	22

6.1 Resultant surface winds, fine grid, global.....	24
6.2a Resultant gradient level wind, observed, tropics, 120°W-60°E....	24
6.2b Resultant gradient level wind, observed, tropics, 60°E-120°W....	24
6.3 Resultant surface streamlines, observed, North America.....	25
6.4 Resultant surface winds, medium grid, global.....	25
7.1 U-component of surface wind, fine grid, Northwest Quarter.....	27
7.2 U-component of surface wind, observed, Northwest Quarter.....	27
7.3 U-component of surface wind, medium grid, Northwest Quarter.....	27
8.1 U-component of surface wind, fine grid, Eastern Hemisphere.....	30
8.2 U-component of surface wind, observed, Eastern Hemisphere.....	30
8.3 U-component of surface wind, medium grid, Eastern Hemisphere.....	30
9.1 V-component of surface wind, fine grid, Northwest Quarter.....	33
9.2 V-component of surface wind, observed, Northwest Quarter.....	33
9.3 V-component of surface wind, medium grid, Northwest Quarter.....	33

10.1 V-component of surface wind, fine grid, Eastern Hemisphere.....	36
10.2 V-component of surface wind, observed, Eastern Hemisphere.....	36
10.3 V-component of surface wind, medium grid, Eastern Hemisphere....	36
11.1 V-component of surface wind, fine grid, equatorial zone.....	39
11.2 V-component of surface wind, medium grid, equatorial zone.....	39
11.3 V-component of surface wind, observed, equatorial zone.....	39

LIST OF TABLES

PAGE

1.1 Summary of SLP and rainfall verification, Northwest Quarter.....	3
2.1 Summary of SLP and rainfall verification, Eastern Hemisphere.....	8
3.1 Summary of SLP and rainfall verification, Southwest Quarter.....	14
4.1 Summary of 7th-layer zonal wind verification, Northwest Quarter..	18
5.1 Summary of 7th-layer zonal wind verification, Eastern Hemisphere.	21
7.1 Summary of surface zonal wind verification, Northwest Quarter....	26
8.1 Summary of surface zonal wind verification, Eastern Hemisphere...	29
9.1 Summary of meridional surface wind verification, NW Quarter.....	32
10.1 Summary of meridional surface wind verification, Eastern Hem.....	35
11.1 Summary of cross-equatorial flow verification.....	38

VERIFICATION OF REGIONAL CLIMATES OF GISS GCM- Part 1: Winter

1. Dec-Jan-Feb, Northwest Quarter

North America: Fine Grid: SLP is too high over the USA, and there is a suspicion that lows are not generated in the lee of the Rockies or along the Gulf coast as they should be. These lows draw moisture from the Gulf of Mexico and create a gradient of increasing rainfall rates from the Plains' states toward the east and southeast. Too few lows or lows that are too shallow would cause too little precipitation over the eastern and southeastern USA. Thus the model shows a precipitation minimum over the southeast USA (less than 1mm/d) instead of the observed maximum of 3mm/d. The mean model SLP and precipitation distributions show that lows do traverse southern Canada and the northeastern US. Thus, simulated winter precipitation over the Great Lakes and New England is quite realistic.

The model rainfall of 2.5mm/d over the Rockies is too rainy. The gradient toward lower rainfall rates is not sharp enough and the orographic rain shadow over the eastern slopes is diffuse. This deficiency is probably a result of the limited model resolution of the high topography.

The SLP troughing and associated precipitation maximum along the Gulf of Alaska coast has been simulated quite well.

Medium Grid: The mean winter model climate over North America is inferior to the fine-mesh version in several respects: The Gulf of Alaska SLP trough is not deep enough, there is a high over the Great Lakes and eastern Canada, there is a trough over Florida. The precipitation pattern is worse in that the gradient over the western US is more diffuse. This supports the idea that this feature is sensitive to model resolution of the topography (see above). The medium grid has, however, more properly given more rain to the southeastern US, although there is slightly too much precipitation along the east coast. More cyclonic activity is apparently being generated here from the Gulf of Mexico to New England.

N. Pacific Ocean:Fine Grid: The Aleutian low and sub-tropical high are represented quite well by the model simulation. The precipitation associated with developing and migrating cyclones over the N. Pacific is simulated as much heavier than observed, but the subtropical minimum off California is fairly realistic.

Medium Grid: This version maintains a much shallower and less realistic Aleutian low, and no subtropical high at all! Precipitation rates lower than 4mm/d are probably more accurate than in the fine grid.

N. Atlantic Ocean:Fine Grid: A spurious high of 1050mb appears over Greenland while the Icelandic trough is displaced to the southeast of its observed position. The swath of precipitation along the trajectory of the North Atlantic lows is geographically well-placed by the model, although rates do not match observations. The precipitation maximum over southern Greenland is somewhat under-represented while the maximum over the western Atlantic is much too rainy, similar to the model verification over the North Pacific. The subtropical anticyclone is realistically represented.

Medium Grid: The winter SLP also shows the 1050mb high over Greenland. However, the Icelandic low is better positioned, although it is too shallow. This version does not show the troughing along the trajectories of the oceanic lows 40°-50°N that appear on the fine grid SLP, implying that cyclonic activity is minimized here. The subtropical ridge generated on the medium grid is less realistic than the fine grid result, being about 5mb shallower than the latter and climatology.

Table 1.1 Summary, verification for Northwest Quarter

<u>North America</u>	<u>Fine Grid (848F9)</u>	<u>Medium Grid (882M9)</u>
Great Plains trough:	barely perceptible	better troughing
SE Alaska trough:	accurate depiction	too shallow
W US high:	4mb too high	4mb too high
Rain max, Gulf states:	depicts minimum	max displaced to SE
Rain gradient, across Rockies:	too diffuse	much more diffuse
<u>North Pacific</u>		
Aleutian trough:	good representation	much too shallow
Subtropical high:	good representation	much too shallow
<u>North Atlantic</u>		
Greenland:	spurious high	spurious high
Iceland low:	displaced to SE	8mb too shallow
Subtropical high:	good representation	much too shallow

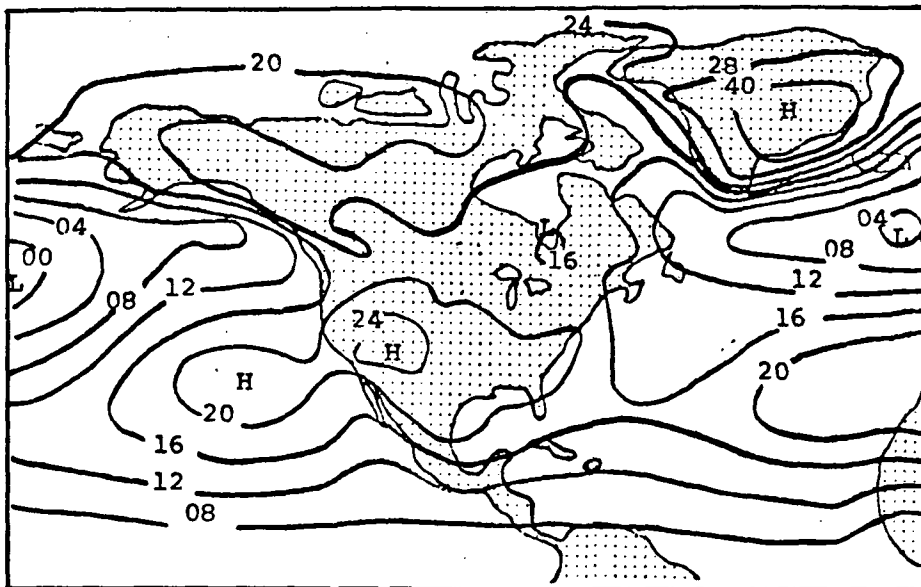


Fig. 1.1 Sea-level pressure (mb-1000), fine grid Winter (Dec-Jan-Feb)

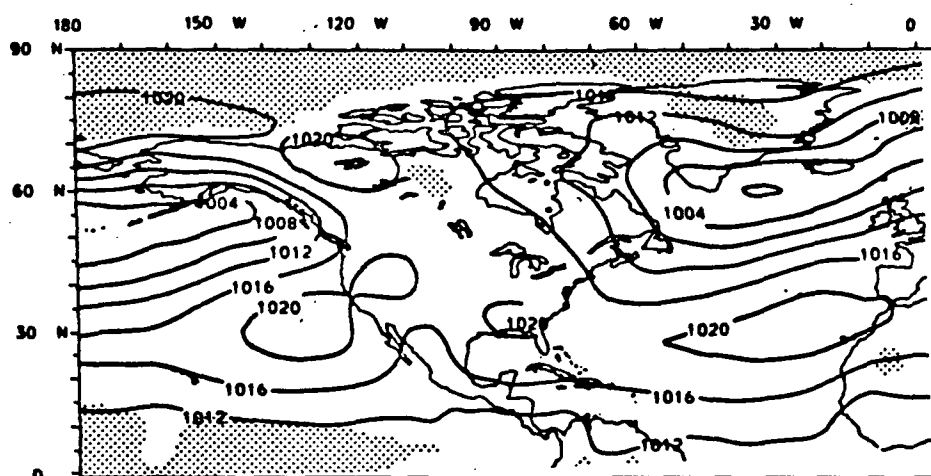


Fig. 1.2 Sea-level pressure (mb), observed Winter (Dec-Jan-Feb)

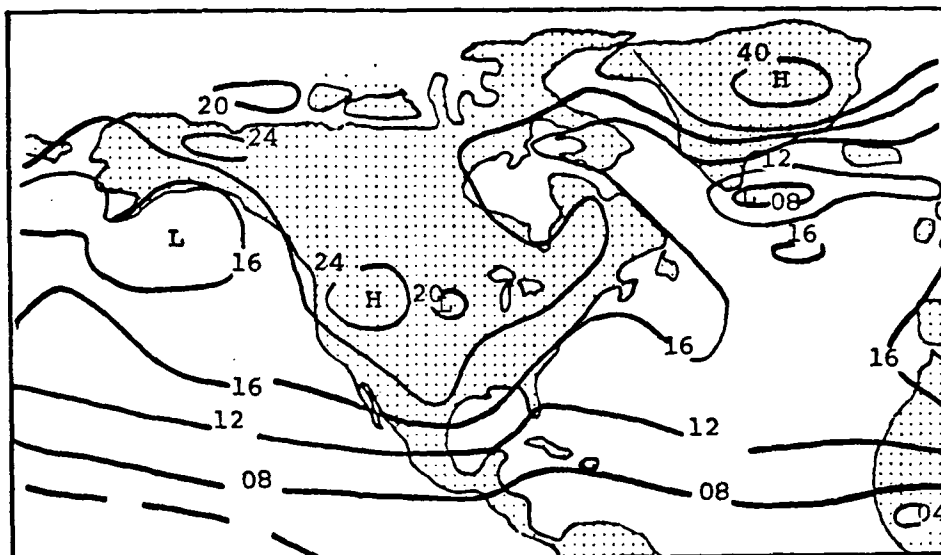


Fig. 1.3 Sea-level pressure (mb-1000), medium grid Winter (Dec-Jan-Feb)

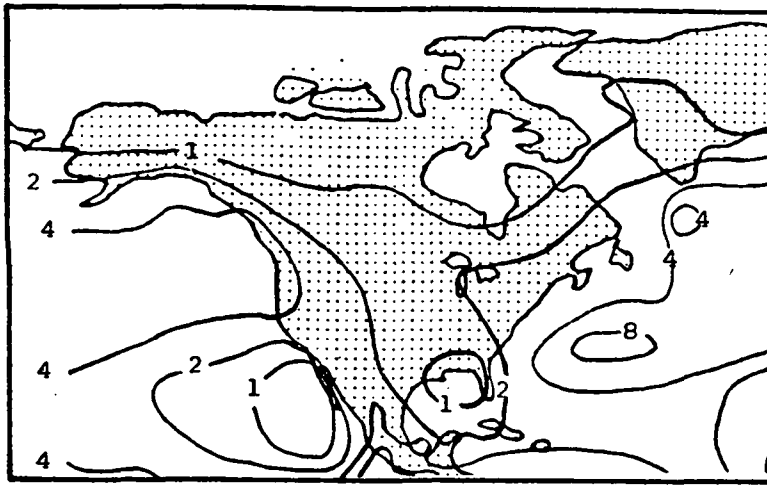


Fig. 1.4 Precipitation rate (mm/day), fine grid, Winter (Dec-Jan-Feb)

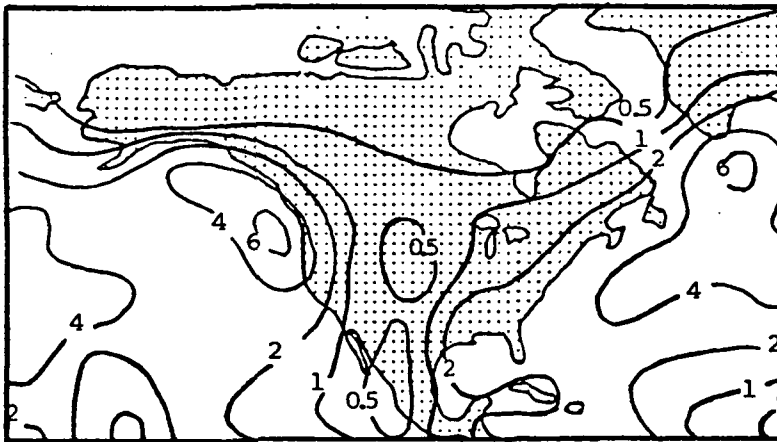


Fig. 1.5a Observed precipitation rate (mm/day), Winter (Dec-Jan-Feb)

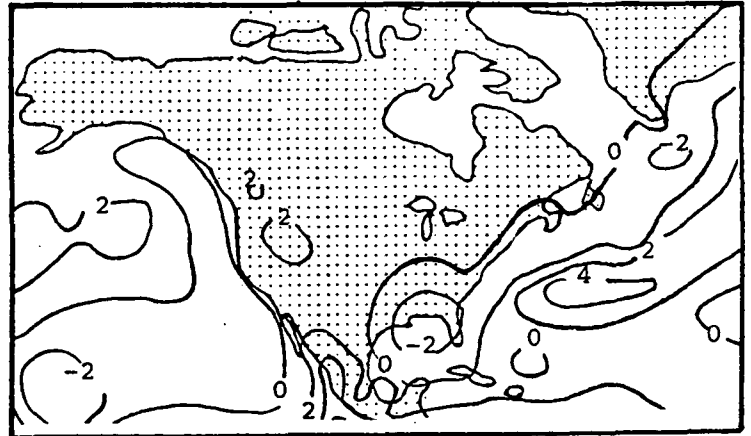


Fig. 1.5b Fine grid model minus observed precipitation (mm/d)

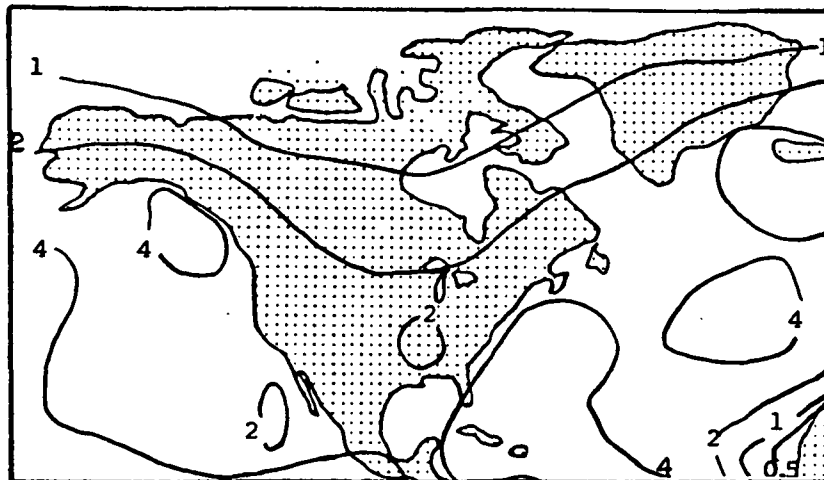


Fig. 1.6 Precipitation rate (mm/day), medium grid, Winter (Dec-Jan-Feb)

2. Dec-Jan-Feb, Eastern Hemisphere

Europe and Africa: Fine Grid: The southwest circulation depicted by the mean winter SLP over Europe is quite realistic, although it is displaced southward of the actual pattern. The simulated SLP maximum over north Africa and the minimum over the Mediterranean Sea are some 5mb too high. Since the low pressure over the southern half of Africa was realistically simulated, the SLP gradient between this region and North Africa is stronger than it should be. The precipitation patterns for the fine grid model correspond fairly well to the observed patterns over Europe and the Mediterranean Sea. Similarly, over most of Africa, the rainfall rates are realistic, except for the excessive values generated along 4°S and over the Horn (Somalia).

Medium Grid: The winter mean SLP does not show a strong northwest-southeast gradient like that verified over Europe for the fine grid. It also does not resolve any closed low over the Mediterranean, although SLP values there and over north Africa are probably more correct than in the fine grid results. The low pressure over south Africa is situated well, although it is a few mb too deep. The precipitation pattern generated by this model version verifies as well over Europe as the fine grid and verifies better along 4°-12°S over Africa by not maximizing the rainfall rate. The medium grid does, however, show a slightly more diffuse isohyet gradient between the dry Sahara and the rainy region to the south. The pattern of desert along the western coast of south Africa and heavy rain to the east over Mozambique and Madagascar is realistic, as in the fine grid simulation.

Asia: Fine Grid: The SLP pattern is too rough over southern Asia (Isobars have been smoothed in Fig. 2.1.), presumably because of the high topography. The SLP over most of the continent is about 6-8mb too high while SLP over the Indian Ocean are some 4mb too low, combining for an excessive gradient over India and southeast Asia. The model shows a good representation of the strong northerlies along the east coast and over Japan between the Siberian high and the north Pacific low. A spurious maximum of 4mm/day of precipitation is indicated over northern India where observations show only about 1mm/day. The rest of Asia is made realistically dry, except for the southeast where the model indicates moderate rainfall in an area observed to be quite dry in winter.

Medium Grid: Isobars are unrealistically unsmooth over almost all of Asia. This includes two deep minima over the Himalayas and over Pakistan that are completely anomalous. The maximum over central Asia is similar to the fine grid result. The precipitation pattern of this model is much less representative, showing rates that are much too high over all of south Asia and parts of central Asia.

Indian Ocean: Fine Grid: The ITCZ trough is properly positioned, but minimum SLP are about 4mb too low. The monsoon low over northern Australia and the subtropical high southwest of Australia are fairly well simulated, although SLP are a few mb too low. While precipitation maxima over Indonesia and New Guinea are realistic, the two model minima between them are spurious as is the line of heavy rainfall along 12°N. The model climatology actually shows a line of minimum along 4°S where the ITCZ rainfall should be. The Australian monsoon rains are too far inland and the model simulates a dry pocket over the northern coast where the heaviest rains should be.

Medium Grid: Results closely parallel those described above except that the Australian monsoon rainfall is grossly underestimated, all of the significantly high rates being confined to the New Guinea region to the north.

Table 2.1 Summary, verification for Eastern Hemisphere

	<u>Fine Grid (848F9)</u>	<u>Medium Grid (882M9)</u>
SLP gradient accross Europe	too strong in south	altogether too weak
Mediterranean low	SLP 4mb too high	SLP slightly too high
North African SLP	4mb too high, excessive SLP gradient	SLP match observations gradient slightly large
Sahara Desert	properly dry	properly dry
Equatorial Africa	too rainy along 4°S	better, lower rainfall
Southern African low	too diffuse	minimum 4mb too low
E-W precip gradient over southern Africa	realistic, but slightly too rainy SW coast	similar to fine grid
Asian high	topographic distortions of SLP, max too high	SLP even more perturbed, max like fine grid
Asian rainfall	spurious max over India, rest realistically dry	unrealistically rainy over southern half
Indian Ocean ITCZ	SLP 4mb too low, good trough axis location, precip max too far north	similar to fine grid
Australian monsoon	precip max too far south	too dry northern Austr.

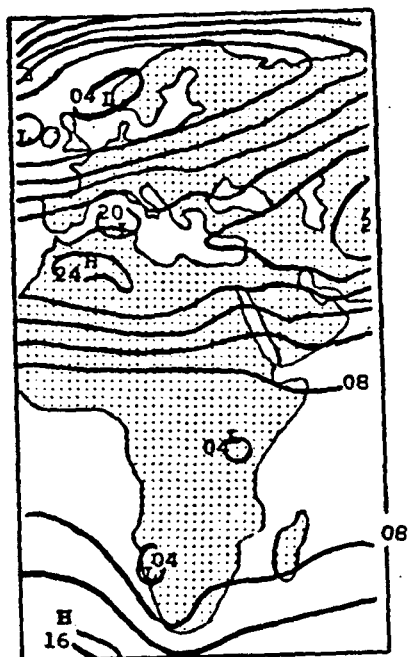


Fig. 2.1 Sea-level pressure (mb-1000), fine grid, Winter

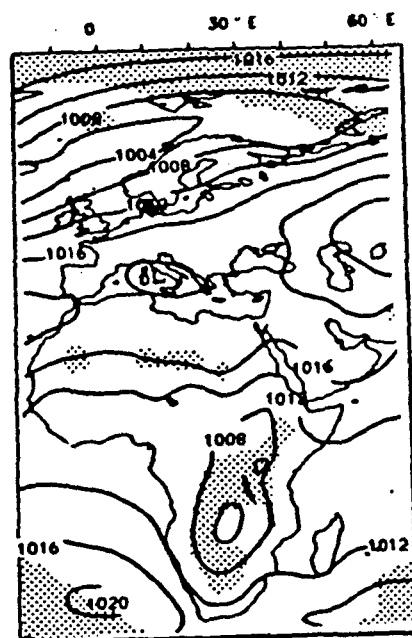


Fig. 2.2 Sea-level pressure (mb), observed, Winter

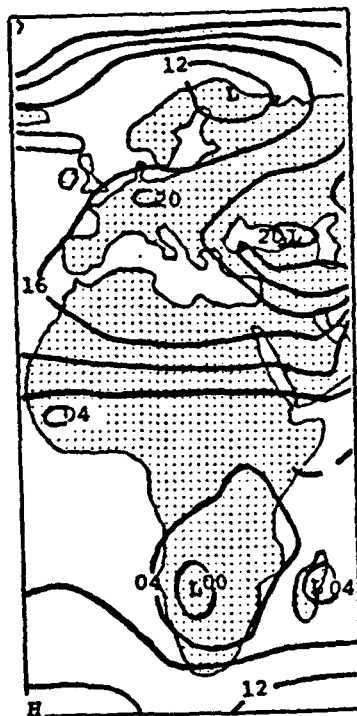


Fig. 2.3 Sea-level pressure (mb-1000) medium grid, Winter (Dec-Jan-Feb)

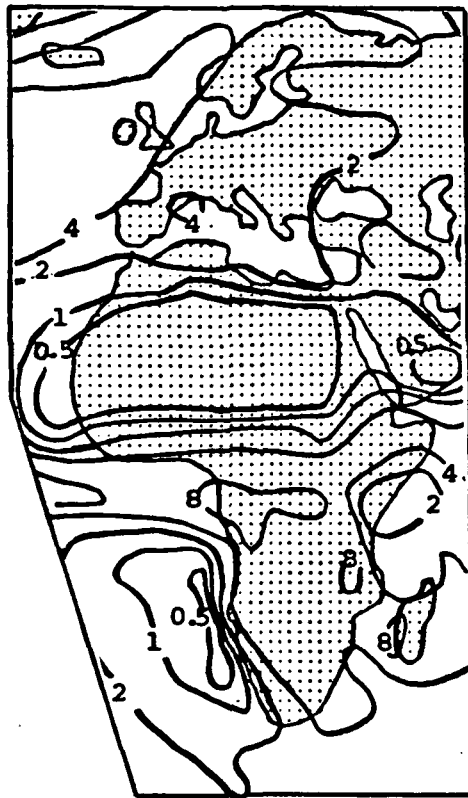


Fig. 2.4 Precipitation rate (mm/day)
fine grid, Winter (Dec-Jan-Feb)

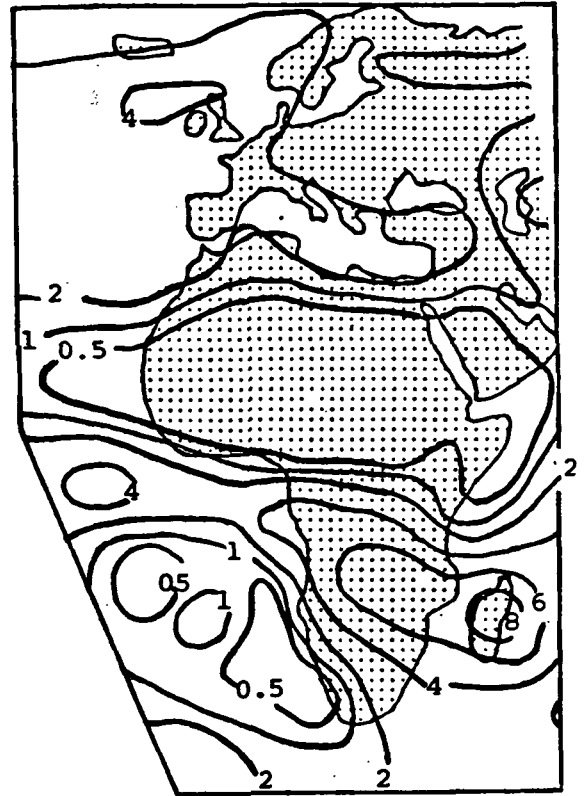


Fig. 2.5a Precip rate (mm/day)
observed, Winter (Dec-Jan-Feb)

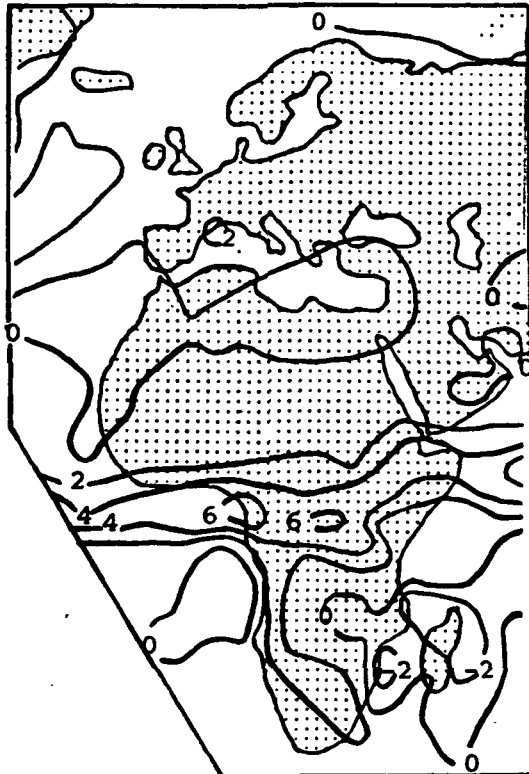


Fig. 2.5b Fine grid model minus
observed precipitation (mm/day)

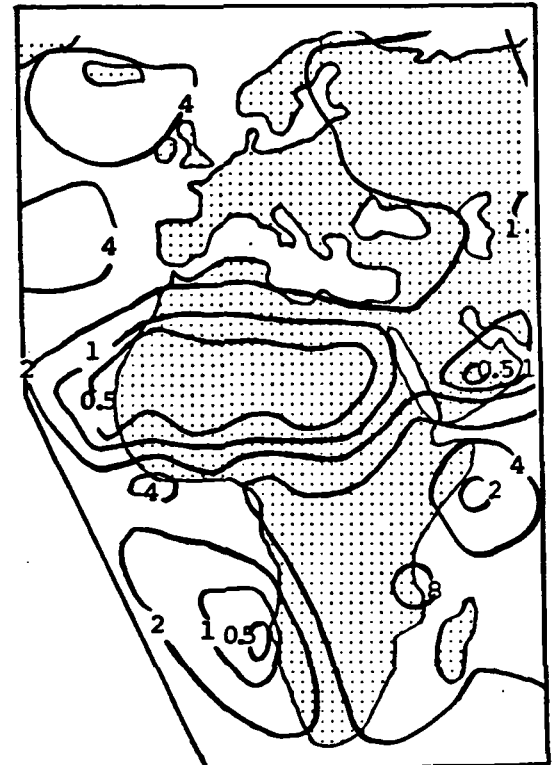


Fig. 2.6 Precip rate (mm/day)
medium grid, Winter (DJF)

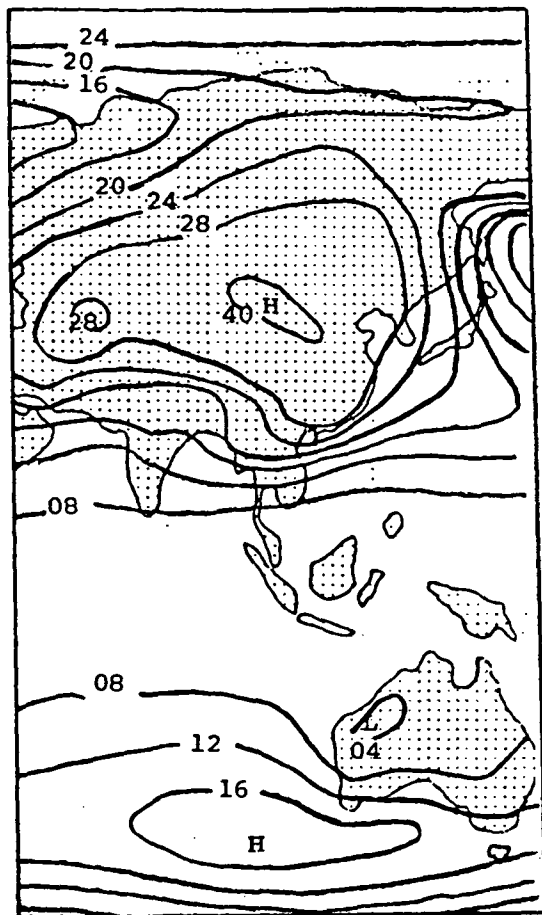


Fig. 2.7 Sea-level pressure (mb-1000)
fine grid, Winter (DJF)

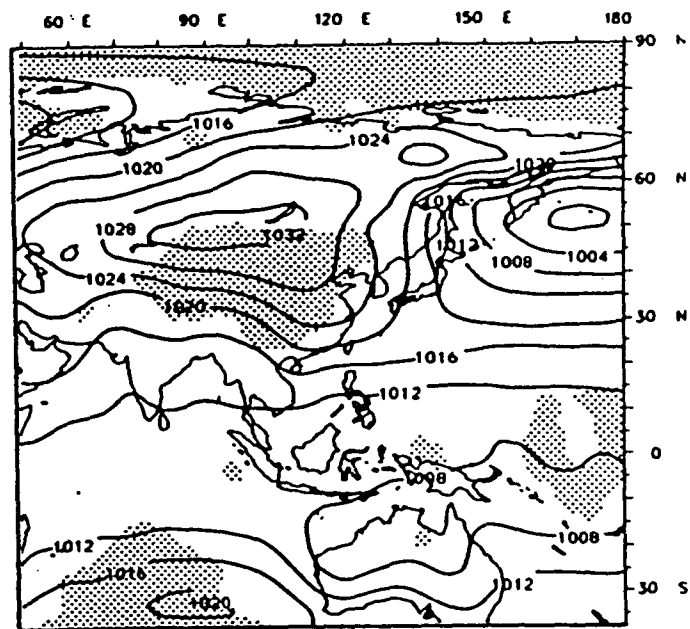


Fig. 2.8 Sea-level pressure (mb)
observed, Winter (DJF)

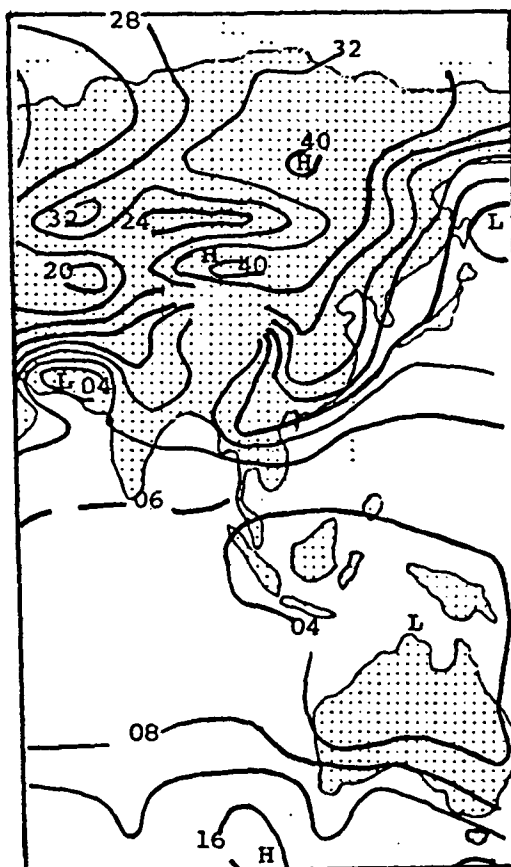


Fig. 2.9 Sea-level pressure (mb-1000), medium grid, Winter (DJF)

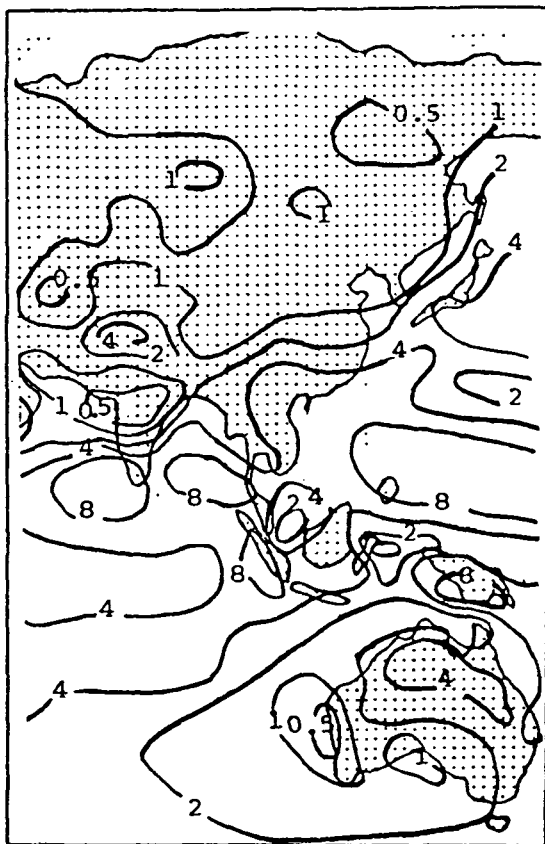


Fig. 2.10 Precipitation rate (mm/day)
fine grid, Winter (Dec-Jan-Feb)

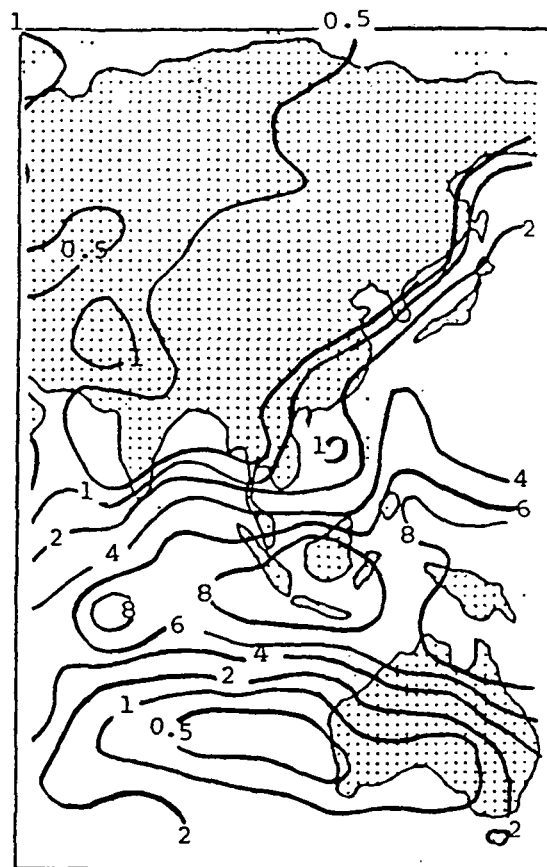


Fig. 2.11a Precipitation rate (mm/d)
observed, Winter (Dec-Jan-Feb)

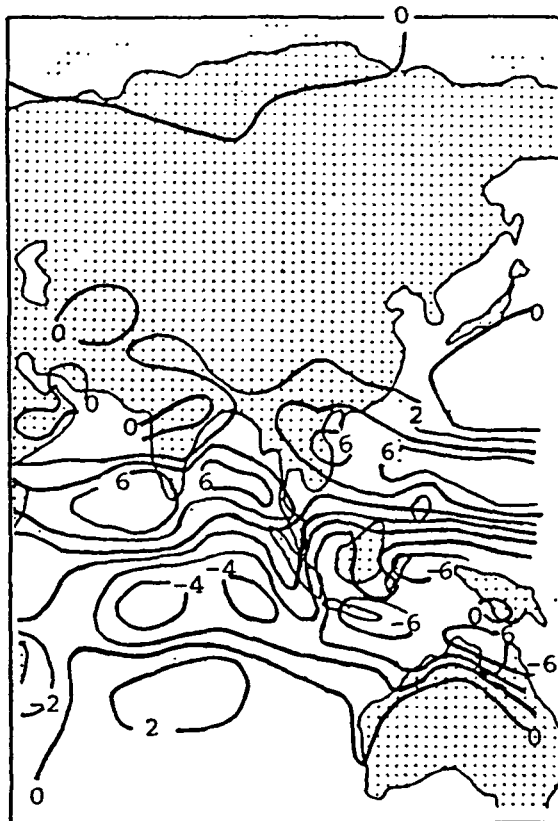


Fig. 2.11b Fine grid minus observed
precipitation rate (mm/day)

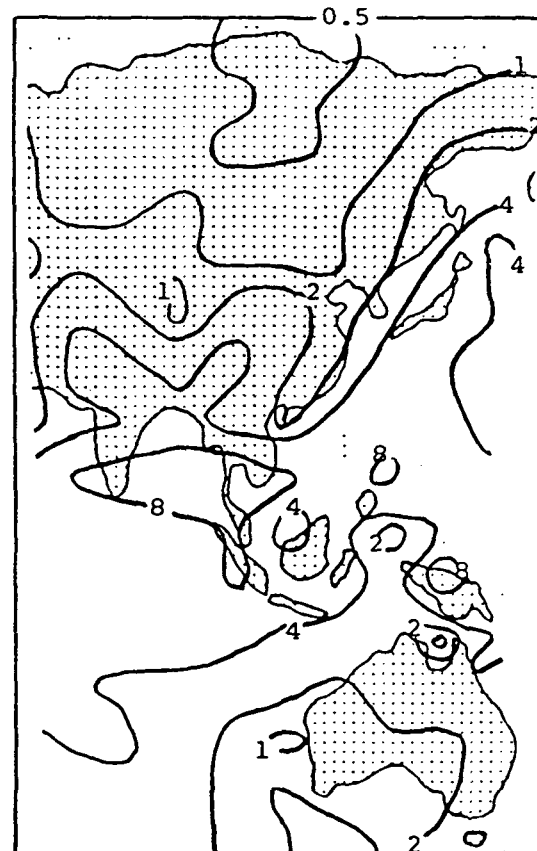


Fig. 2.12 Precipitation rate (mm/d)
medium grid, Winter (Dec-Jan-Feb)

3. Dec-Jan-Feb, Southwest Quarter

South America: Fine Grid: Although the SLP low center has been well placed, the central pressure is about 5mb too low. The precipitation maxima skirt the periphery of the observed maximum giving errors of +6 to -2mm/day. Still, the minima along the west coast are realistic.

Medium Grid: Performance parallels that of the fine grid with two exceptions:

1. The dry area off the west coast penetrates inland too far at mid-continent creating discrepancies of -4mm/day.
2. A small dry area along the northern coast is nicely simulated by the medium grid but not the fine grid.

Tropical and

South Pacific: Fine Grid: Central pressures within the ITCZ are some 4mb too low although the trough position is realistic. The subtropical high is perhaps 3-4mb shallower than the observed. Several very realistic precipitation features are in evidence over much of the tropical Pacific, including the maxima along 12°S and 4°N over the central and eastern portions separated by a minimum near the equator. Errors of up to 6mm/day in the precipitation rate occur where the depicted minimum is too narrow. Spurious heavy rainfall is depicted near Central America (12°N) in an area that is observed as quite arid.

Medium Grid: The SLP has the same shortcomings as the fine grid over the tropical and S. Pacific. The precipitation patterns are also similar except that the heaviest rains here are less extreme and therefore less realistic, except along 12°N where the error is somewhat smaller.

Table 3.1 Summary, verification for Southwest Quarter

<u>South America</u>	<u>Fine Grid (848F9)</u>	<u>Medium Grid (882M9)</u>
Continental low pressure	about 5mb too low	similar to fine grid
Equatorial precip max	diffuse, underestimated	larger underestimate
North coast precip min	not depicted	realistic depiction
<u>Tropical Pacific</u>		
ITCZ trough	4mb too low	4mb too low
Double precip max	4°N max realistic, 12°S max displaced nwd, minimum too narrow	maxima not extreme enough
12°N spurious precip	16mm/d too high near Central America	Same error in kind, less extreme
<u>South Pacific</u>		
Subtropical high	4mb too shallow	6mb too shallow

Fig. 3.3 Sea level pressure (mb-1000), medium grid, Winter (Dec-Jan-Feb)

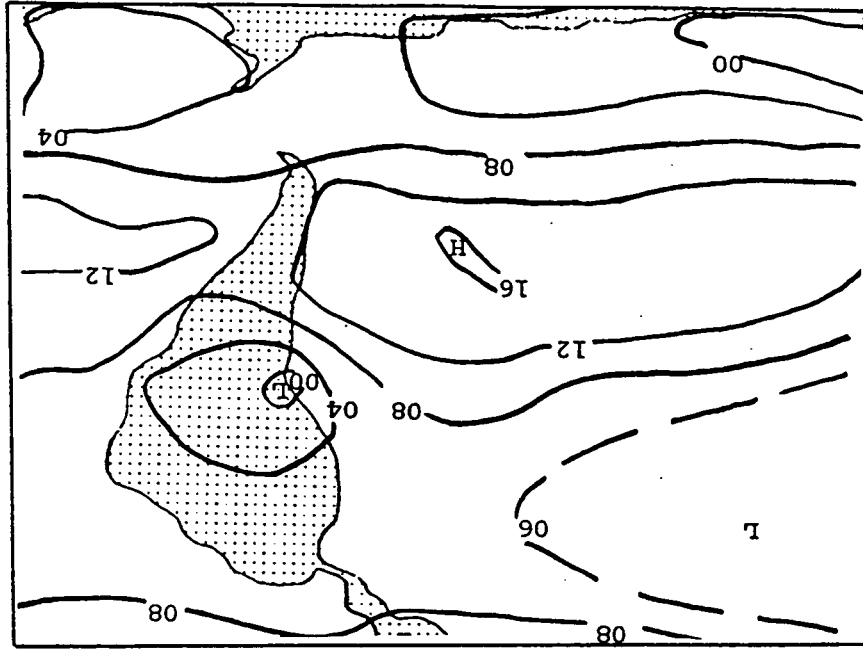


Fig. 3.2 Sea-level pressure (mb), observed, Winter (Dec-Jan-Feb)

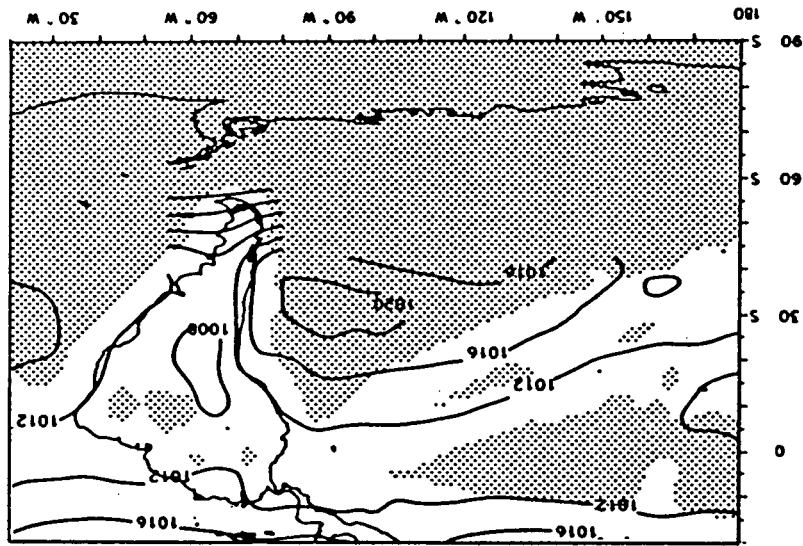
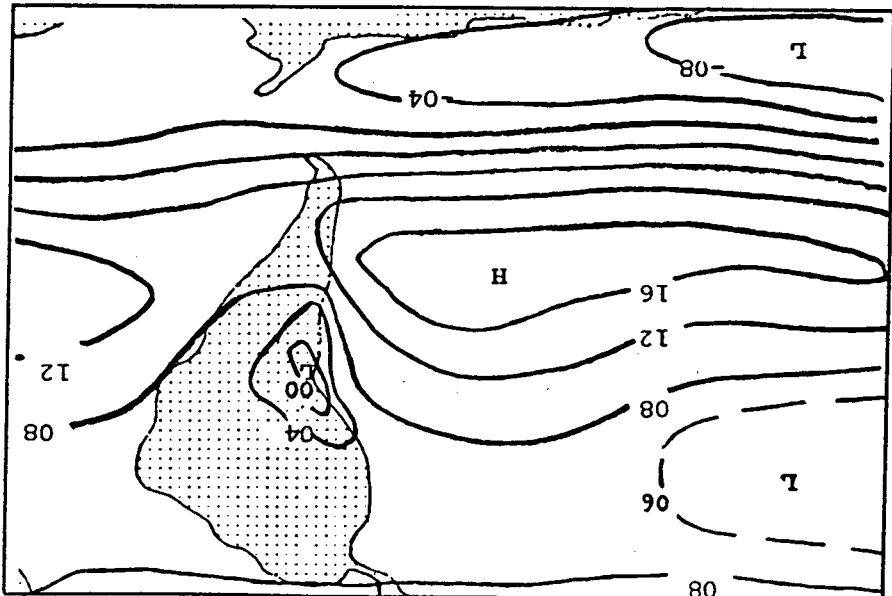


Fig. 3.1 Sea-level pressure (mb-1000), fine grid, Winter (Dec-Jan-Feb)



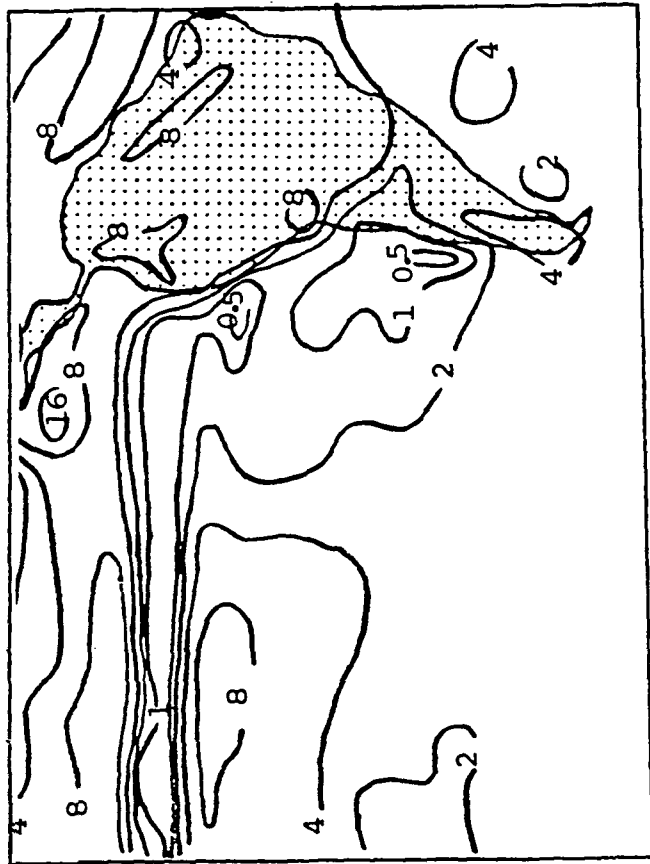


Fig. 3.4 Precipitation rate (mm/day), fine grid
Winter (Dec-Jan-Feb)

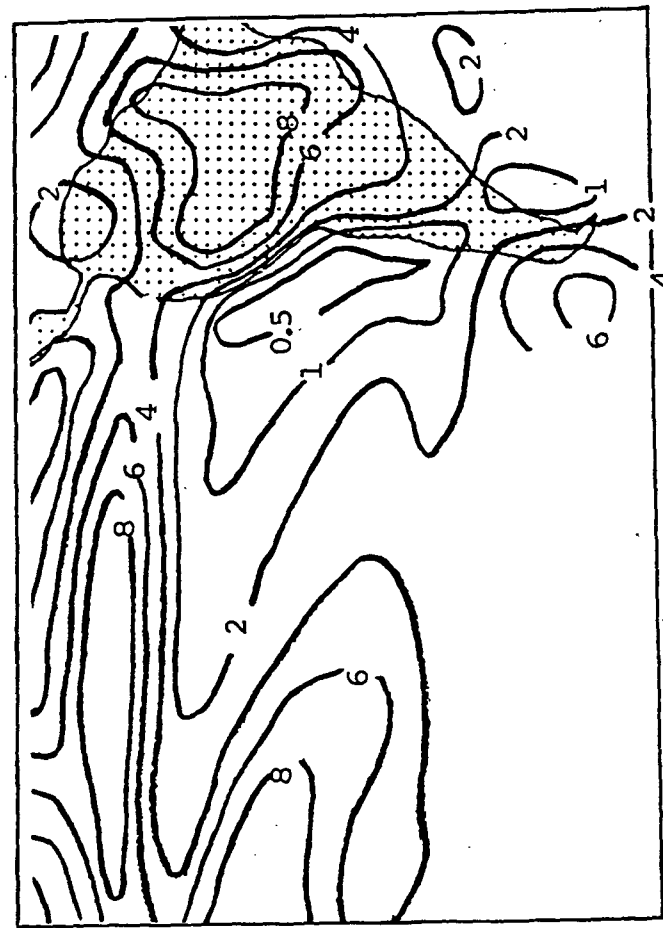


Fig. 3.5a Precipitation rate (mm/day), observed
Winter (Dec-Jan-Feb)

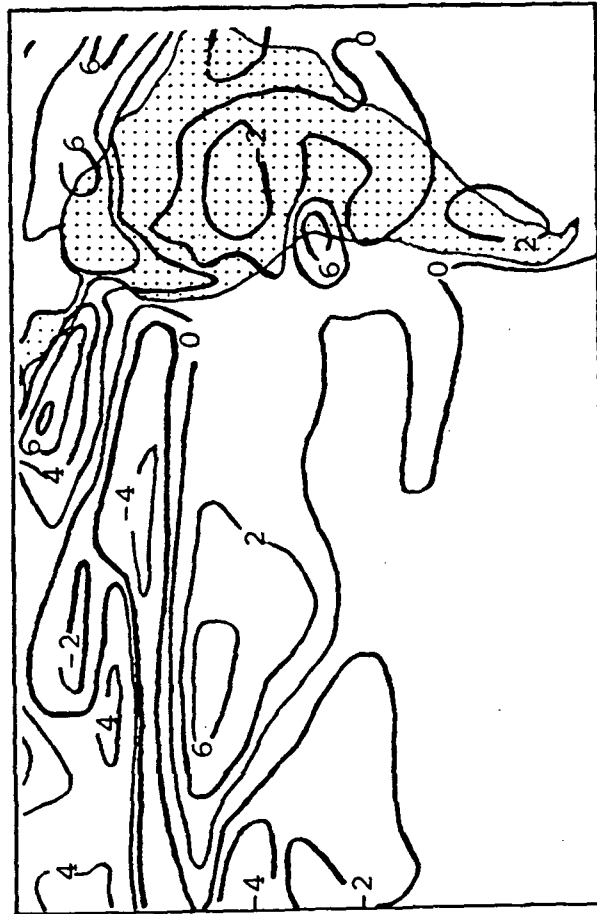


Fig. 3.5b Fine grid model minus observed
precipitation (mm/day)

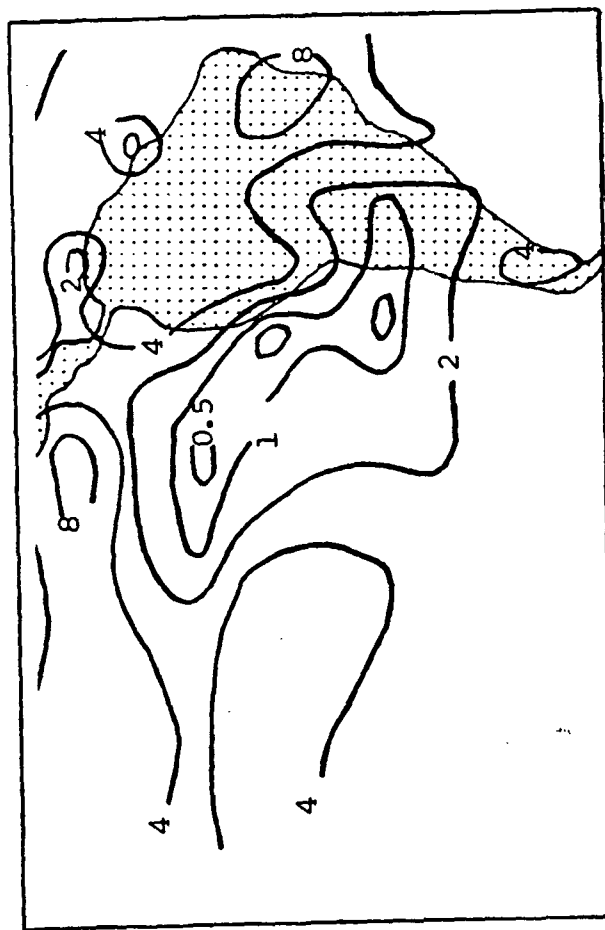


Fig. 3.6 Precipitation rate (mm/day), medium grid
Winter (Dec-Jan-Feb)

4. U-Component of the 7th-layer wind: Dec-Jan-Feb, Northwest Quarter

The only winds aloft saved for model climatologies are at this level. For the mean global surface pressure, the 7th layer corresponds to approximately 200mb. At this level, the u-component represents most of the total wind vector. The analyses of wind component observations are reproduced from Global Atmospheric Circulation Statistics by A. Oort (NOAA, 1983) and represent means from 1963-1973.

Fine Grid: The maxima define the average position of the jet stream, or some combination of the polar and subtropical jets. In the model, the seasonal maximum over North America is greater than 50m/s, centered at 32°N over the southeast USA. The axis of maximum wind speed extends along 32°N over the USA but shifts to 38°N over the eastern Pacific Ocean. Over the Atlantic Ocean the jet is oriented SW-NE, reaching to about 45°N over the eastern half. Observations show that the position of the maximum over the southeastern US is realistic although the model's computed magnitude is perhaps too high. (The mean of this component for the entire 30°N latitude circle is about 10m/s too strong in the model.) The northward shift of the axis of maximum wind speed over the oceans is not verified by these observations. The model maximum over the Pacific Ocean is also some 15m/s stronger than the observed.

Medium Grid: The maxima here are weaker than in the fine grid and they are therefore closer to the observed values. The zonal wind for this model is only about 5m/s weaker than the observed over the United States and the subtropical Pacific Ocean but perhaps some 10m/s too weak over the Atlantic Ocean along 30°N.

Table 4.1 Summary, verification of 7th-layer winds, Northwest Quarter

	<u>Fine Grid (848F9)</u>	<u>Medium Grid (882M9)</u>
Maximum SE USA	good position, 10m/s too fast	diffuse max, speeds OK
Pacific Ocean maximum	8° too far north, 15m/s too fast	8° too far north, 5m/s too slow
Atlantic Ocean	mid latitude speeds too fast, subtropical speeds too slow (jet axis toward SE, not NE)	10m/s too slow 30°N jet, reasonable elsewhere

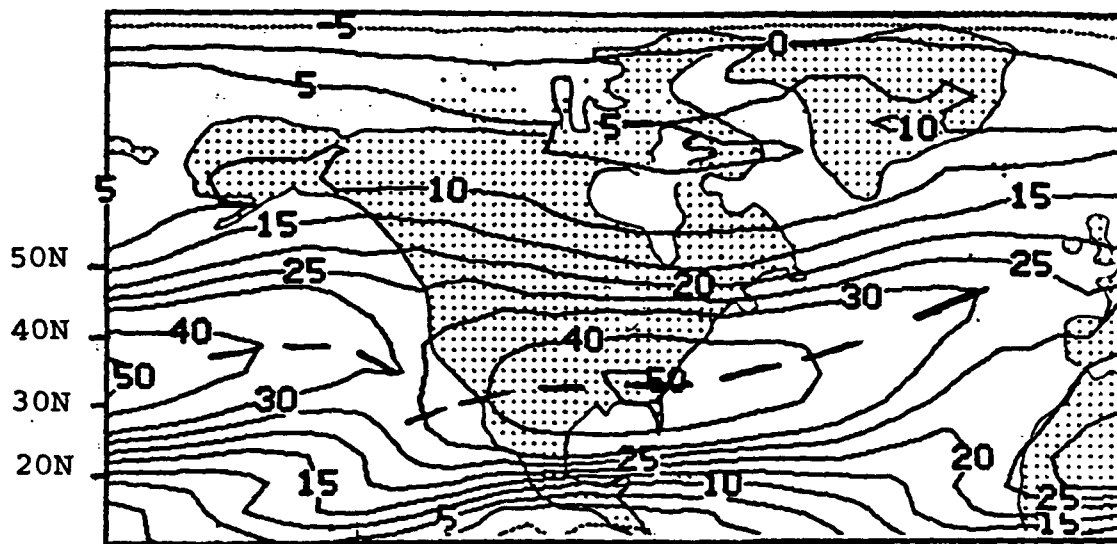


Fig. 4.1 U-component of 7th-layer wind (m/s), fine grid
Winter (Dec-Jan-Feb)

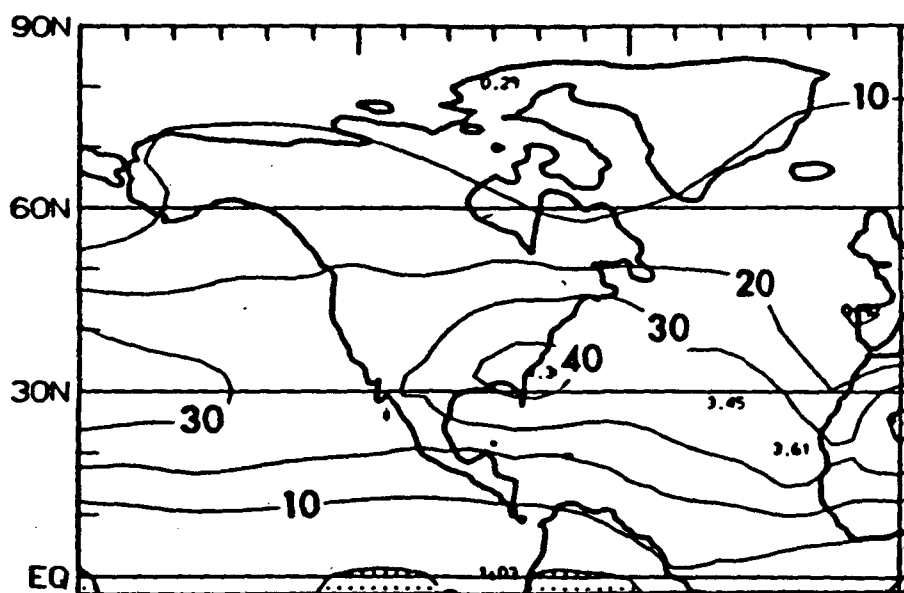


Fig. 4.2 U-component of 200mb wind (m/s), observed
Winter (Dec-Jan-Feb)

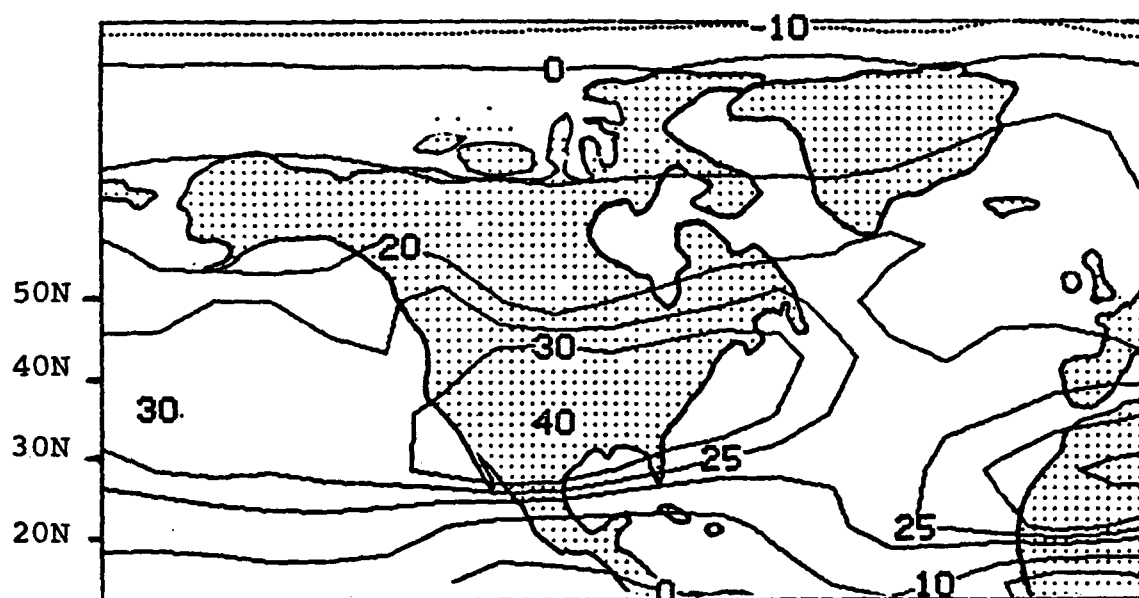


Fig. 4.3 U-component of 7th-layer wind (m/s), medium grid
Winter (Dec-Jan-Feb)

5. U-Component of the 7th-layer wind: Dec-Jan-Feb, Eastern Hemisphere

Fine Grid: The latitude of the model's westerly jet is realistically alligned along 28°N over Africa and Asia with maximum speeds close to the observed. The overall maximum is accurately situated over southern Japan although it is perhaps 10m/s too fast. A checkerboarding of isotachs over western Asia probably indicates some computational problems. The transition to easterlies is correctly made at tropical latitudes, and the speed maxima are quite reasonable. New Guinea should be entirely under easterlies, however, not under a $U=0$ isotach. The axis of the Southern hemisphere westerly jet is also well simulated along 45°S , but maxima are perhaps 10m/s too high.

Medium Grid: The jet over north Africa is simulated quite well, but it shifts too far north over Asia. A spurious speed minimum over southwest Asia interrupts the west-to-east continuity of the flow. In the east, the maximum is more than 10m/s too weak. The minimum over China is unrealistic and may reflect the influence of high topography over south Asia. The band of tropical easterlies is shifted too far north: the maximum over Africa at 8°S is depicted at 4°N and a secondary maximum is shown over southern India which should be under westerly flow. Moreover, on the southern side of the tropical belt, model mid-latitude westerlies already encroach on 10°S latitude which is observed to be under the tropical easterlies according to Dec-Jan-Feb means. The southern hemisphere jet shows reasonable speeds, but it is too far north by one grid interval (8°) at most longitudes.

Table 5.1 Summary, verification of 7th-layer winds, Eastern Hemisphere

	<u>Fine Grid (848F9)</u>	<u>Medium Grid (882M9)</u>
Westerly jet N. Hemis.	excellent representation	perturbed over Asia
Maximum near Japan	10m/s too fast	15m/s too slow
Tropical easterlies	excellent, except too far north over western Pacific	too far north entire E. Hemis.
Westerly jet S. Hemis.	position good, 10m/s too fast	8° too far north, speeds reasonable

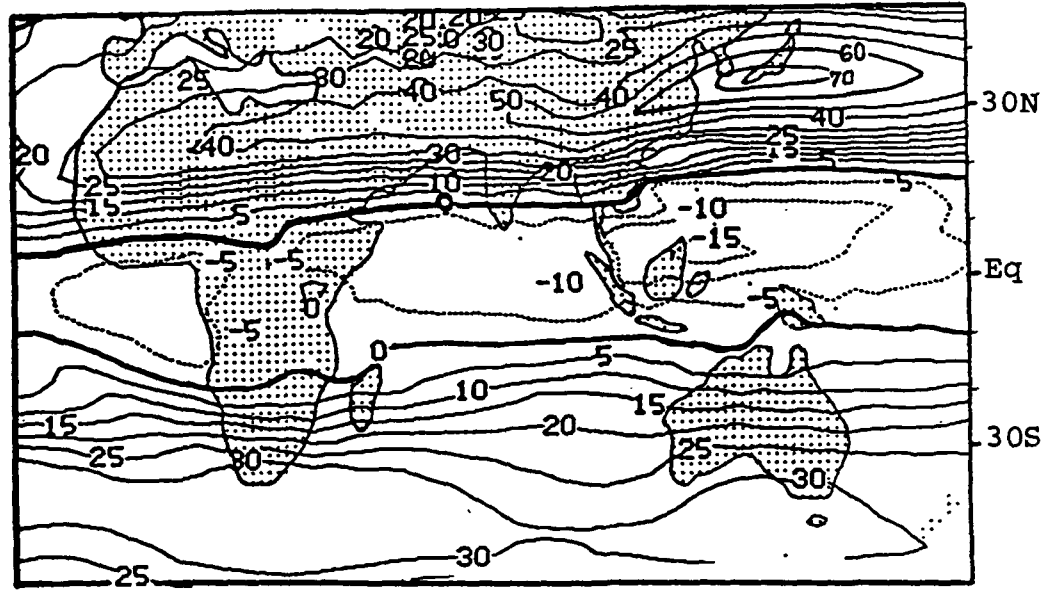


Fig. 5.1 U-component of 7th-layer wind (m/s), fine grid, Winter (DJF)

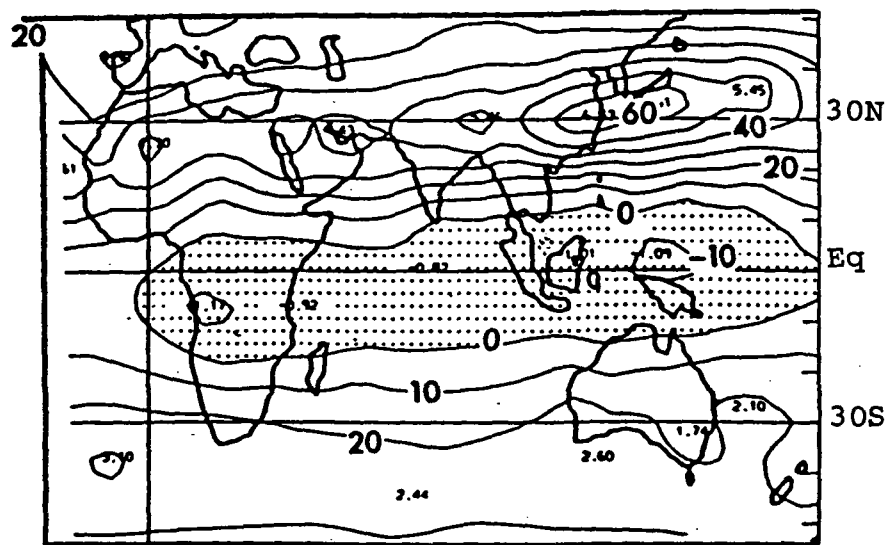


Fig. 5.2 U-component of 200mb wind (m/s), observed, Winter (DJF)

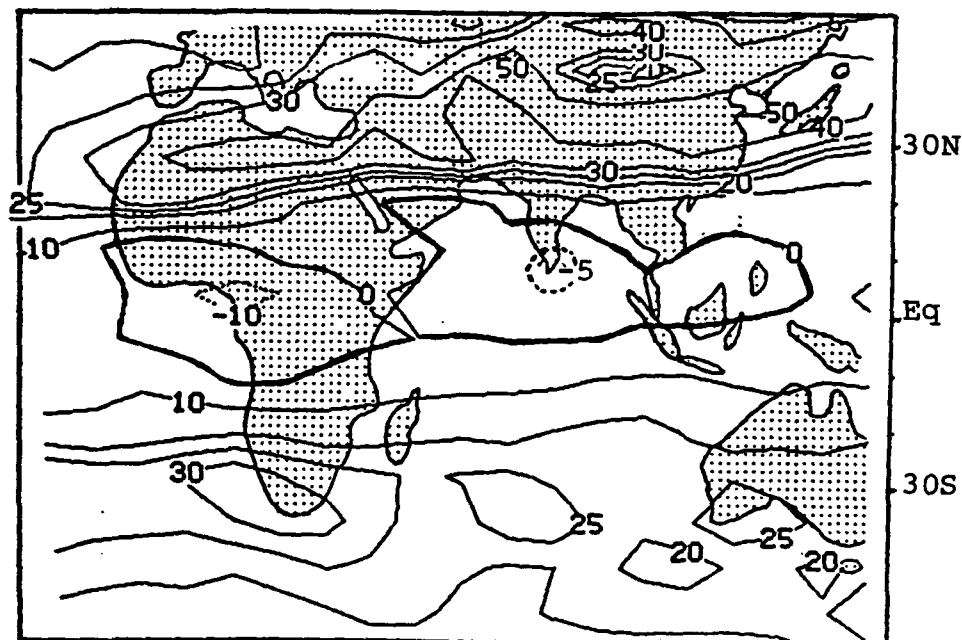


Fig. 5.3 U component of 7th-layer wind (m/s), medium grid, Winter (DJF)

6. Resultant surface wind

The models' resultant surface winds for the three winter months are represented by vectors plotted at each grid box center. These charts show the simulated flow patterns at a glance and they can be compared qualitatively to the streamflow analyses for the observed gradient level wind (tropical latitudes; Atkinson and Sadler, 1970) and to the analysis of surface flow over North America and adjacent oceans (Climates of North Amer., Bryson and Hare, 1974). A more quantitative verification that relates to the mean zonal and meridional components of the surface wind follows.

7. U- component of the surface wind: Dec-Jan-Feb, Northwest Quarter

Fine Grid: The mean westerly component that the model simulates over the United States is about 2m/s too strong. It is also overestimated over parts of the North Atlantic Ocean, although the general pattern of maxima of 4-5m/s over the central ocean is quite realistic. Over the eastern North Pacific Ocean, the maximum is only about 1m/s too high, but over the central ocean, the overestimate larger. The small area of very strong easterlies simulated near Central America is spurious and is probably related to the spurious precipitation maximum that the model depicts in this area. The transition to the easterly trade winds along 30°N corresponds well to the observed analysis as does the maximum of 6-7 m/s near 10°N over the Atlantic; the model's trades in the North Pacific are about 2m/s too weak.

Medium Grid: The westerlies are everywhere weaker than in the fine grid and this offers a more realistic regime for the United States. Over the oceans, however, model values are much too low and the model maxima are too far north. The transition to the easterly trades is about 10° too far north over the North Pacific Ocean and the speed maximum near 10°N is about 4m/s too weak. The spurious east wind here mimicks the performance of the fine grid. The 30°N latitude of the 0-line over the North Atlantic Ocean as well as the axis of strongest easterly trades are well placed although the latter are some 2-3m/s too weak.

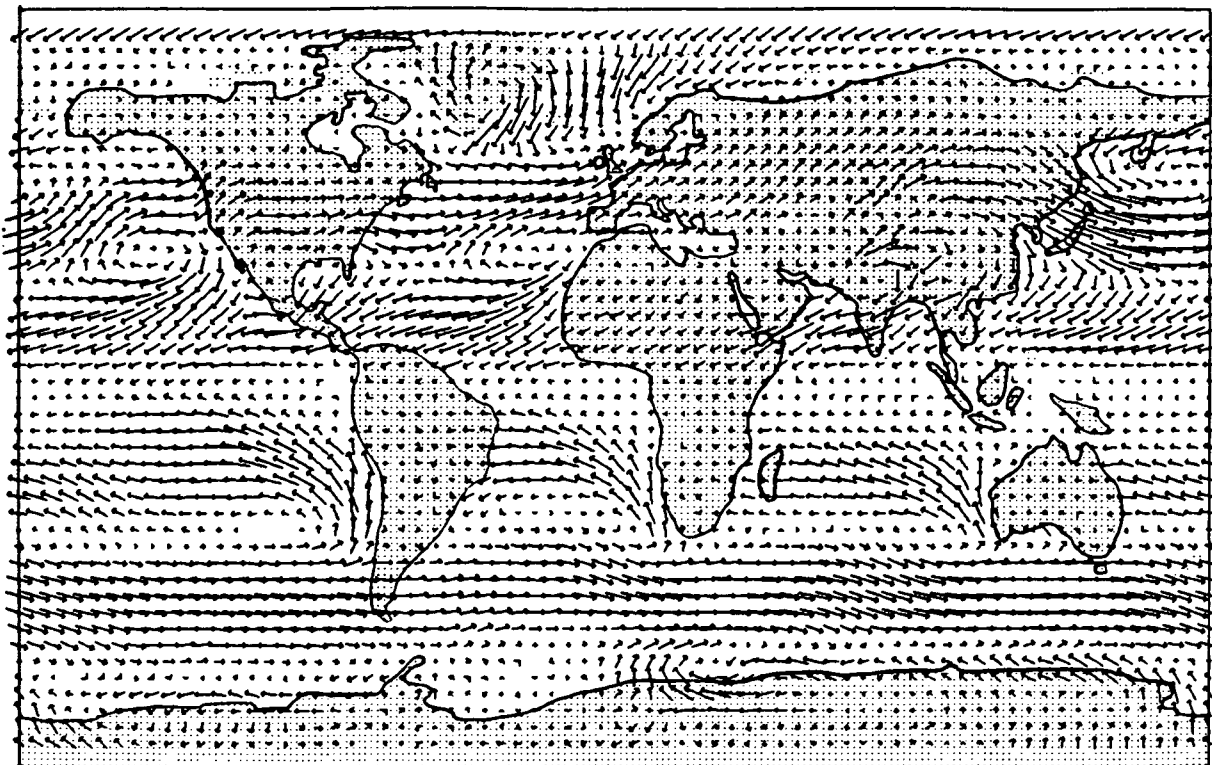


Fig. 6.2a

RESULTANT GRADIENT LEVEL WIND - JANUARY

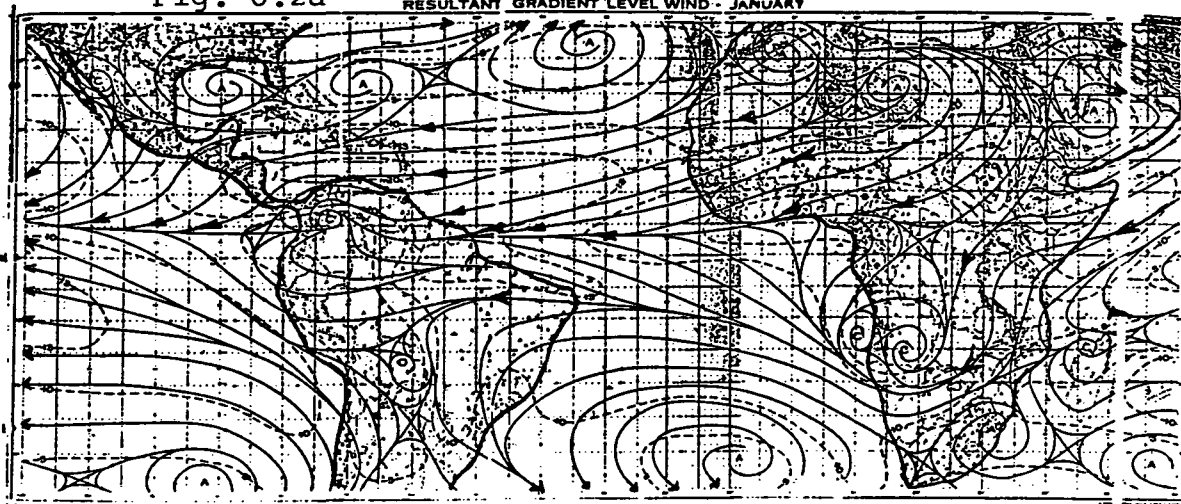
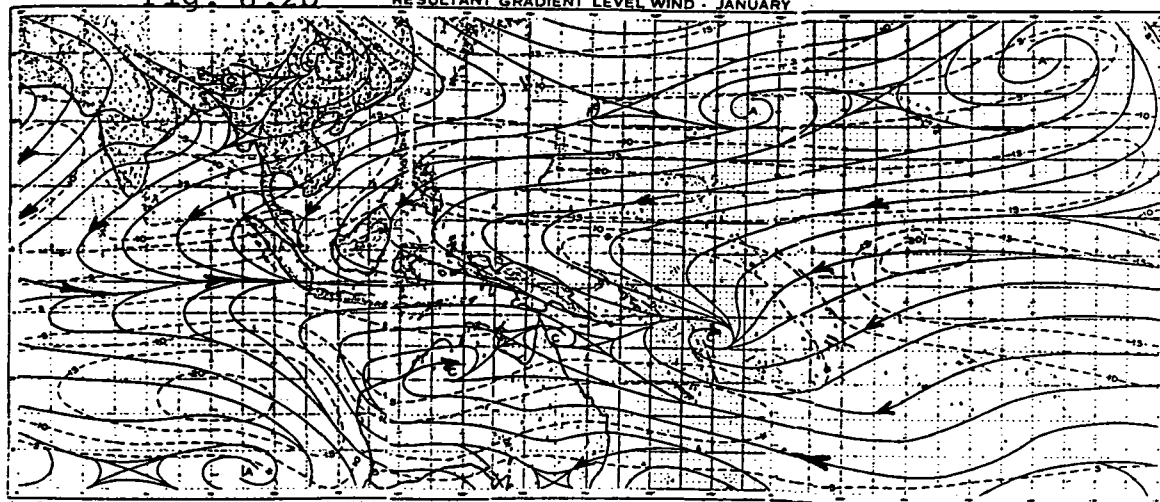


Fig. 6.2b

RESULTANT GRADIENT LEVEL WIND - JANUARY



ORIGINAL PAGE IS
OF POOR QUALITY

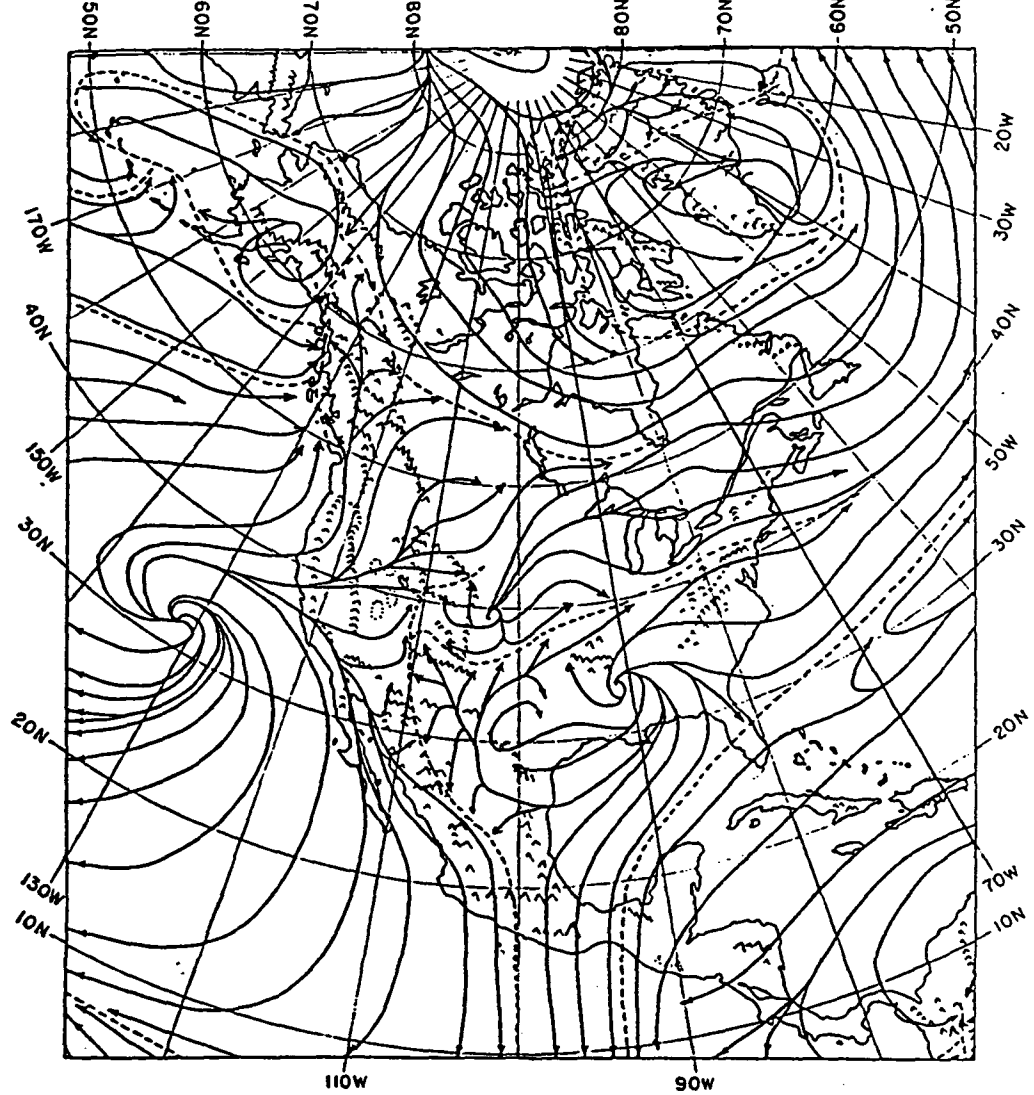


Fig. 6.3 Resultant surface streamlines for January (after NAVAIR, 1966).

Fig. 6.4 SURFACE WIND DJF

(Medium Grid Model) 882 M9

20 (M/S) reference: ———

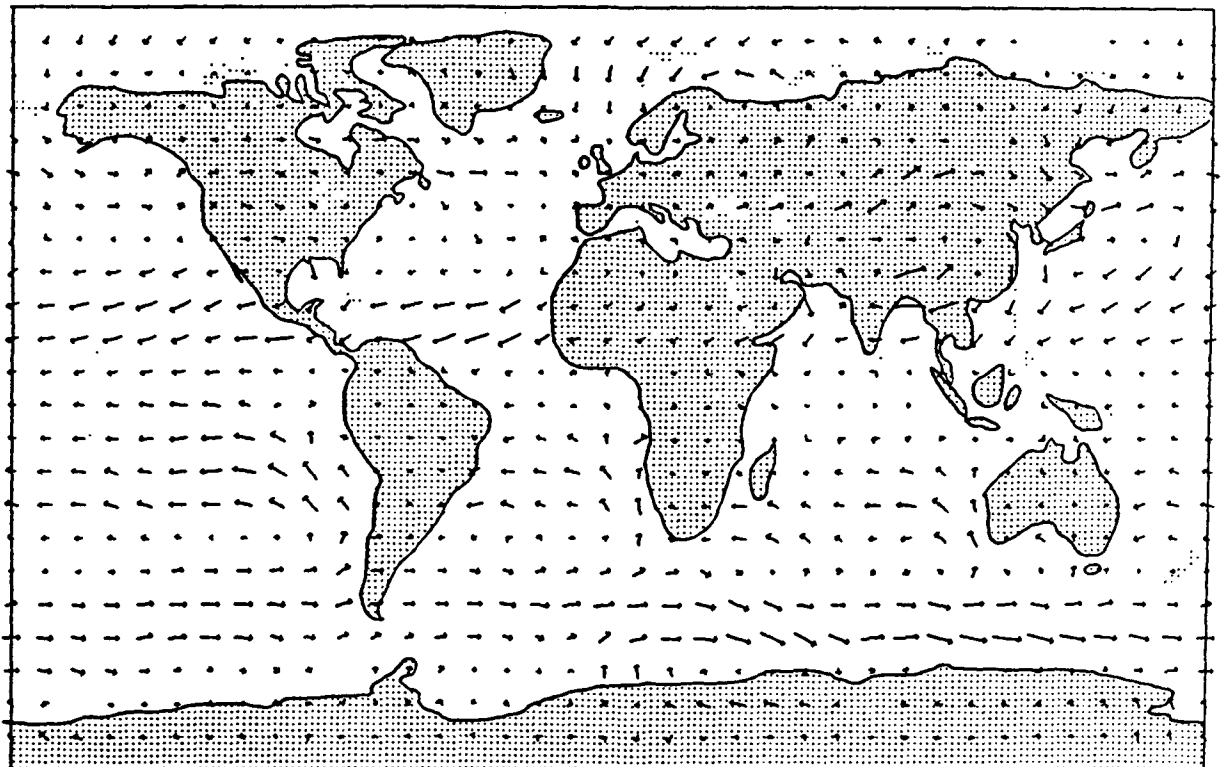


Table 7.1 Summary, verification of zonal surface winds, Northwest Quart.

	<u>Fine Grid (848F9)</u>	<u>Medium Grid (882M9)</u>
Continental USA	2m/s too strong	close to observed
N. Pacific max	1-2m/s too strong, axis well situated	2m/s too weak, axis too far north
N. Atlantic max	good representation	too weak and too northerly
Pacific trades	well situated but 2m/s too weak	begin too far north, max 4m/s too weak
Atlantic trades	quite realistic	max 2-3m/s too weak

ORIGINAL PAGE IS
OF POOR QUALITY

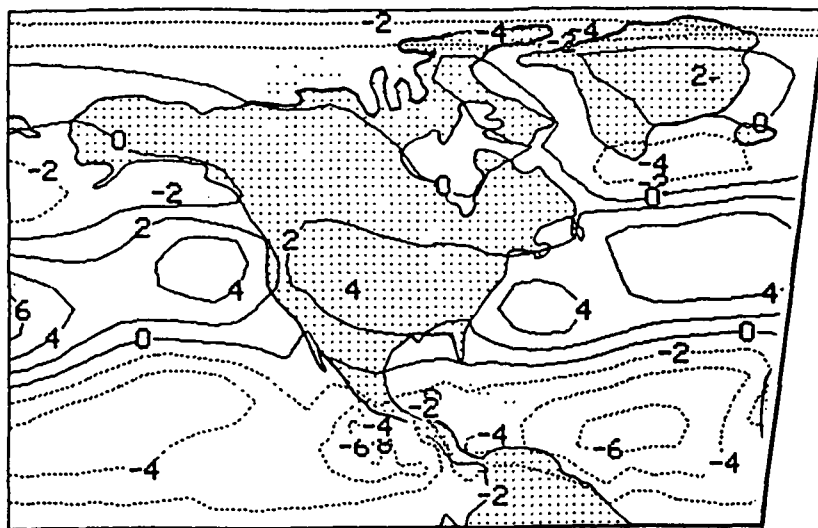


Fig. 7.1 U-component of surface wind (m/s), fine grid
Winter (Dec-Jan-Feb)

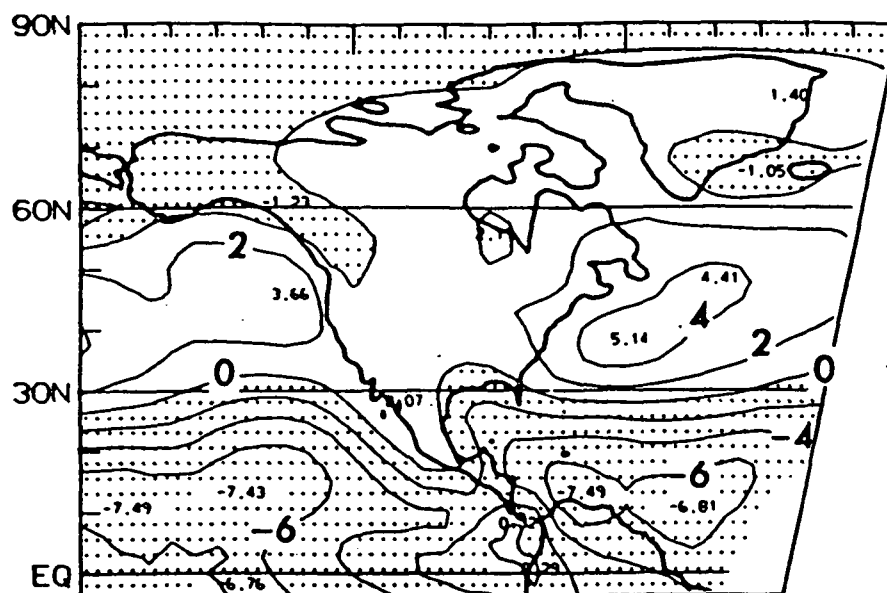


Fig. 7.2 U-component of surface wind (m/s), observed
Winter (Dec-Jan-Feb)

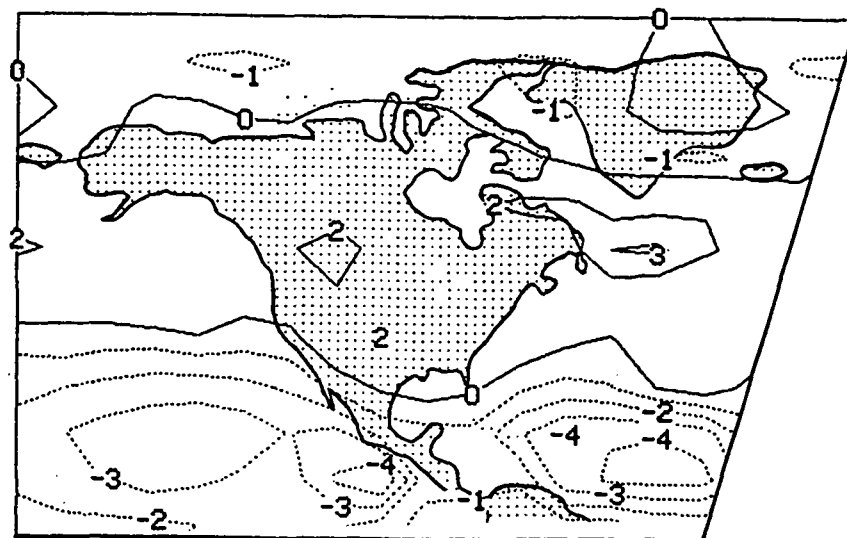


Fig. 7.3 U-component of surface wind (m/s),
medium grid, Winter (Dec-Jan-Feb)

8. U- component of the surface wind: Dec-Jan-Feb, Eastern Hemisphere

Fine Grid: The model's strong SLP gradient over Europe has caused westerlies that are somewhat stronger than observed. However, the relatively high zonal wind speeds over the central Mediterranean are realistic. Unfortunately, the model climate does not extend these westerlies eastward far enough to include the Sinai Peninsula and Israel. Easterlies are conspicuously absent in the model climatology over Eastern Europe and southwestern Asia. These winds are sandwiched between the anticyclonic circulation over Asia and the low pressure trough over the Mediterranean Sea. The model's discrepancy results from the erroneous ridging of high pressure over Syria and southern Turkey, areas that actually experience considerable cyclonic activity during the winter. The maximum of wind speed over the Himalayas is obviously a model response to the high topography, but it is not representative of the observed synoptic circulation. On the other hand, the maximum east of Japan does represent observed accelerations of surface flow around the North Pacific cyclone although the model is about 3m/s too windy.

Bands of easterlies are nicely simulated near 10°N and 20°S from the Pacific Ocean, across the Indian Ocean to Africa. These model easterlies are too weak over the North Pacific and the South Indian Ocean, but are close to the analyzed values over the South Pacific and the North Indian Ocean except for a small area of simulated excess near India. Hooking of the northeast monsoon winds as they cross the equator creates a rather strong westerly component along 0°-10°S that does not show up in the model field because model northerlies do not cross the equator into the South Indian Ocean or the South Pacific.

The model's mid-latitude westerlies over the Southern Hemisphere are quite realistic.

Medium Grid: The zonal wind is almost everywhere weaker than in the fine grid representation. This constitutes an improvement only over Europe. The easterlies of the North and South Pacific and the South Indian Ocean and the mid-latitude westerlies along 50°S are all considerably underestimated. This version does, however, show a weak band of westerly flow along 4°S that was missing in the fine grid.

Table 8.1 Summary, verification of zonal surface winds, Eastern Hemis.

	<u>Fine Grid (848F9)</u>	<u>Medium Grid (882M9)</u>
Europe	U is 1-2m/s too large	U verifies well
Mediterranean	realistic max, Tunisia; westerlies missing over southeastern corner	too weak overall; westerlies missing over SE corner
SW Asia easterlies	entirely missing	entirely missing
Spurious max-Himalayas	6m/s	4m/s
U max near Japan	3m/s too strong	3m/s too weak
Subtropical easterlies 10°N and 20°S	too weak N. Pacific and S. Indian Oceans	generally much too weak, fine grid better
Equatorial westerlies	entirely missing	weaker than observed
S. Hemisphere "	realistic	about 3m/s too weak

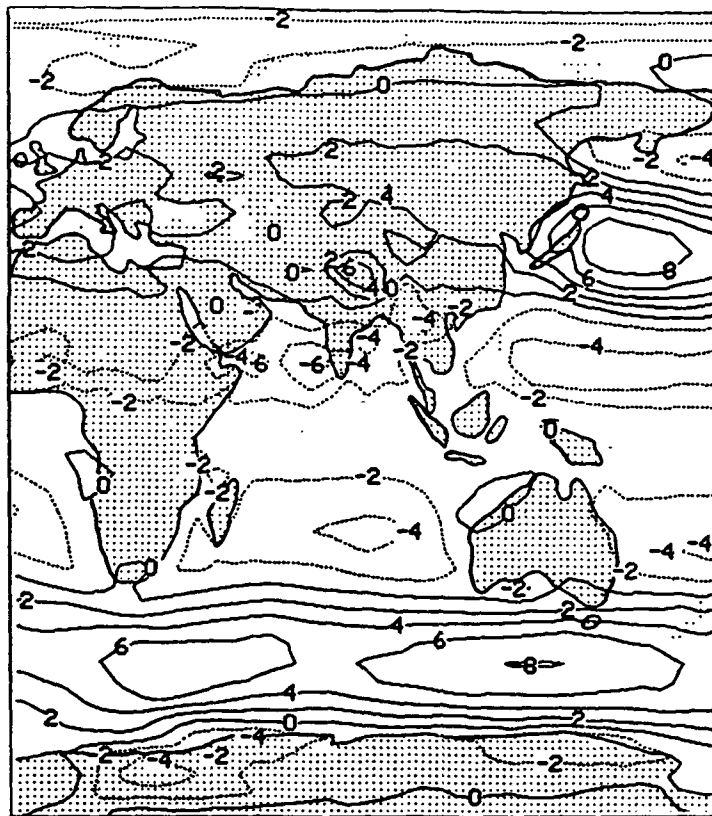


Fig. 8.1 U-component of surface wind (m/s), fine grid, Winter (DJF)

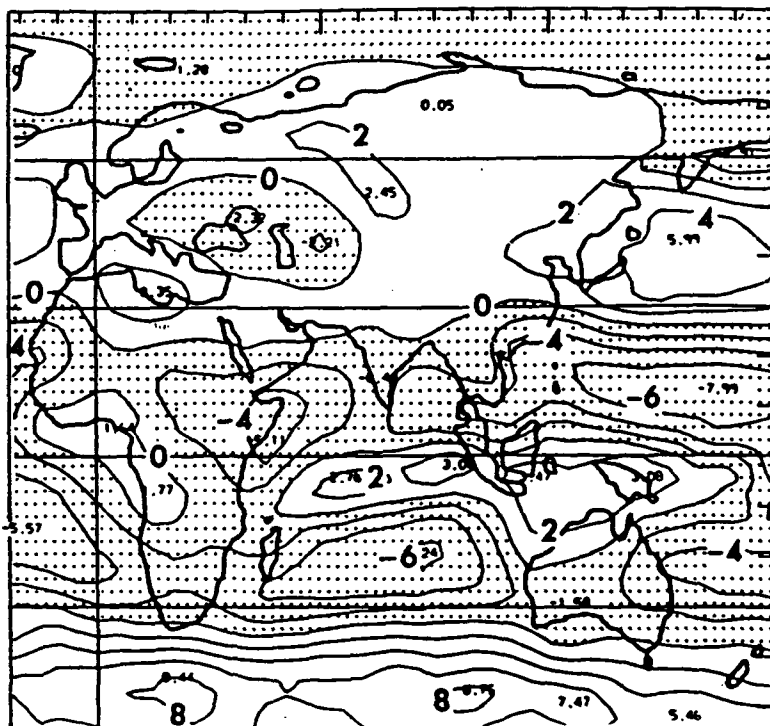


Fig. 8.2 U-component of surface wind (m/s) observed, Winter (Dec-Jan-Feb)

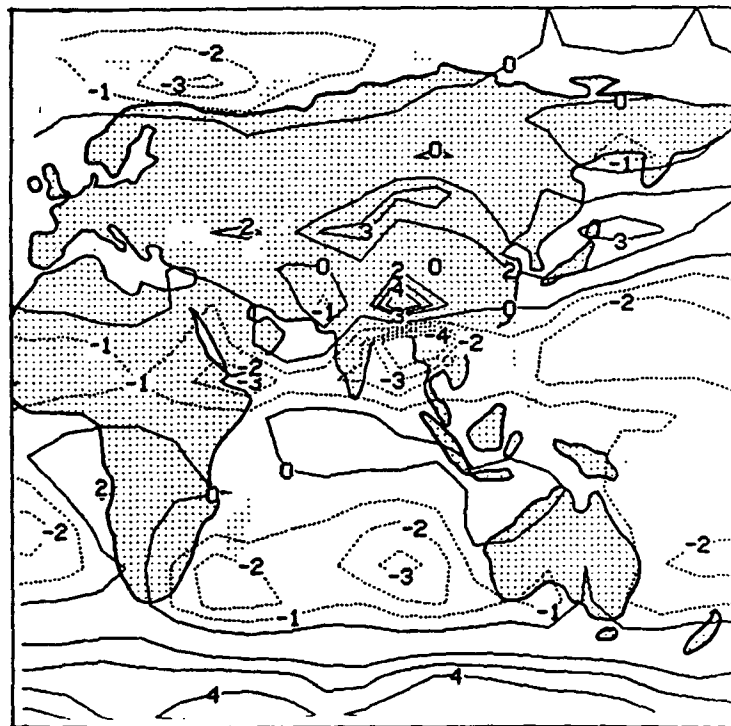


Fig. 8.3 U-component of surface wind (m/s), medium grid, DJF

9. V- component of the surface wind: Dec-Jan-Feb, Northwest Quarter

Fine Grid: The simulated meridional winds over the North American continent are very weak, excluding the area of southerly winds over the northwestern United States. Observations support this depiction except for the strong northerlies over northeast Canada that the model does not show. The southerlies at the west coast as well as those further west over the Pacific are somewhat stronger than observed. Northerly flow that is also part of the North Pacific anticyclonic circulation, is modeled a bit too far off-shore westward of Mexico and it is slightly weaker than observed. Northerly winds of 3m/s over the Yucatan (Mexico) are realistic, but not the hiatus of $V=0$ along the Mexican coast that indicates completely zonal flow there.

The model shows strong anticyclonic circulation over Greenland and Iceland in response to the spuriously high SLP over the former. The pattern of northerlies over the western North Atlantic Ocean and southerlies over central and eastern portions verifies quite well. The strong northerlies around the Atlantic high are well-placed near northwest Africa although simulated values are somewhat weaker than observed, as over the North Pacific.

Medium Grid: The only strong meridional winds over North America are 2-3m/s northerlies over the Gulf of Mexico and the Yucatan (Mexico). Observations of $V < -2\text{m/s}$ are confined to southern Mexico and Central America. The northerlies of northeast Canada are not represented in this model climatology but weak southerlies do appear along the west coast of the continent, mistakenly extending however, as far south as Baja. Northerly flow southeast of the oceanic highs is even more deficient than for the fine grid. Southerly components are missing from other oceanic areas over which they are observed. Strong northerlies in the model east of Greenland probably derive from the spurious high generated over Greenland also in this model version.

Table 9.1 Summary, verification of meridional surface winds, NW Quarter

	<u>Fine Grid (848F9)</u>	<u>Medium Grid (882M9)</u>
NE Canada northerlies	not represented	not represented
NW USA southerlies	slightly too strong	too weak, too far south
N. Pacific southerlies	2m/s too strong	not represented
W. Mexico/Pacific northerlies	mistakenly interrupted west of Mexico	3m/s too weak over Pacific
Greenland	spurious anticyclonic	spurious anticyclonic
northerlies W. Atlant.	realistic	similar to fine grid
southerlies E. Atlant.	realistic	almost nil
northerlies SE N.Atl.	2m/s too weak	3m/s too weak

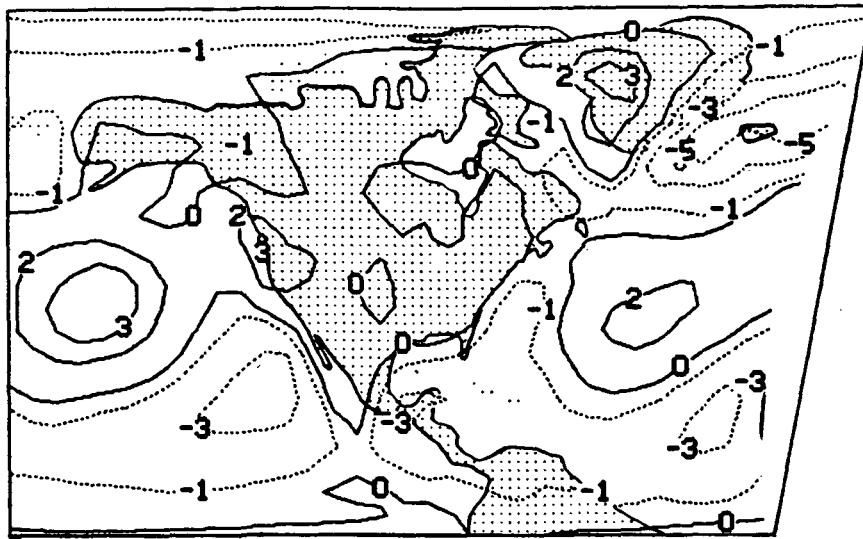


Fig. 9.1 V-component of surface wind (m/s), fine grid, Winter (DJF)

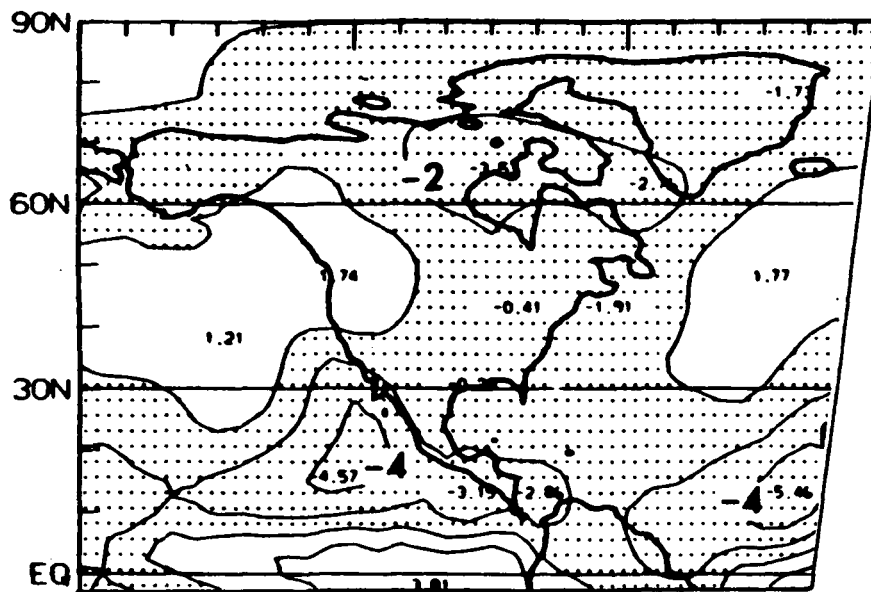


Fig. 9.2 V-component of surface wind (m/s), observed, Winter (DJF)

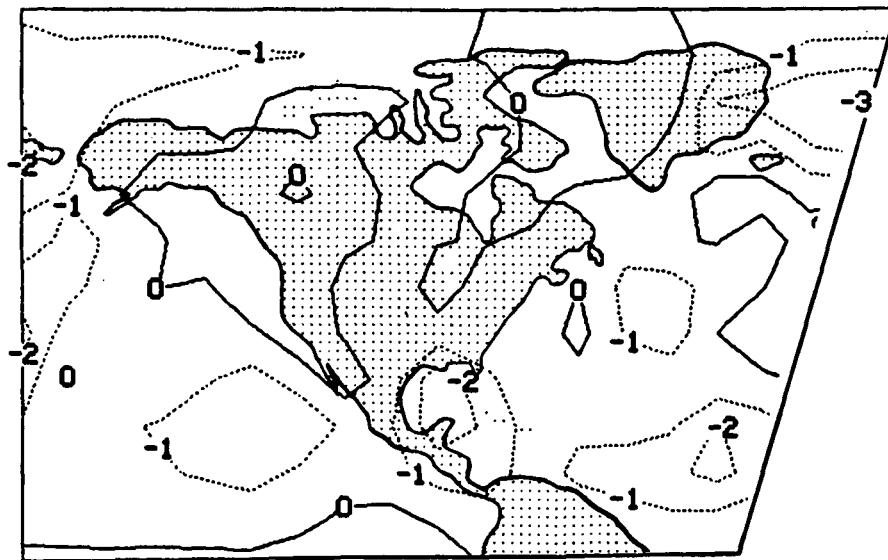


Fig. 9.3 V-component of surface wind (m/s), medium grid, Winter (DJF)

10. V-component of the surface wind: Dec-Jan-Feb, Eastern Hemisphere

Fine Grid: Observations have the southerly component of the surface wind confined to the northern half of Europe and Asia. The model shows a southerly component exceeding 2m/s over most of southwestern and central Europe and over several areas in southwestern, central and southern Asia. Northerlies are more correctly depicted near the eastern coast of Asia although the maximum speeds are somewhat too weak. The Indian Ocean is realistically divided into a northerly regime near South Asia and a southerly regime south of the equator. The northerlies over the Arabian Sea and northeastern Africa and the southerlies near western Australia and near southwest Africa are about 2m/s too weak. In both cases these southerlies do not extend far enough over the continental areas.

Medium Grid: Southerlies are far too extensive over Europe and Asia. Northerlies along the east coast of Asia are realistic, even if slightly under-strength, except for an interruption northeast of Japan. While the north winds over the Arabian Sea are perhaps 2-3m/s too weak, they are not depicted at all over most of the North Indian Ocean. Southerlies, some 2-3m/s too weak, are however in place west of Australia and southwest Africa. As in the fine grid, they are missing or very weak over the continental coastal areas.

Table 10.1 Summary, verification of meridional surface winds, E. Hemis.

	<u>Fine Grid (848F9)</u>	<u>Medium Grid (882M9)</u>
northerlies, S. Europe and S. Asia	missing, except SE Asia and India	missing, except SE Asia and SW Asia
northerlies W. coast of Asia	2m/s too weak	2m/s too weak, interrupted NE of Japan
southerlies east of S. Hem. highs	2m/s too weak, not extensive enough	2-3m/s too weak, not extensive enough
northerlies, Arabian Sea and NE Africa	2m/s too weak	1-3m/s too weak, not extensive enough

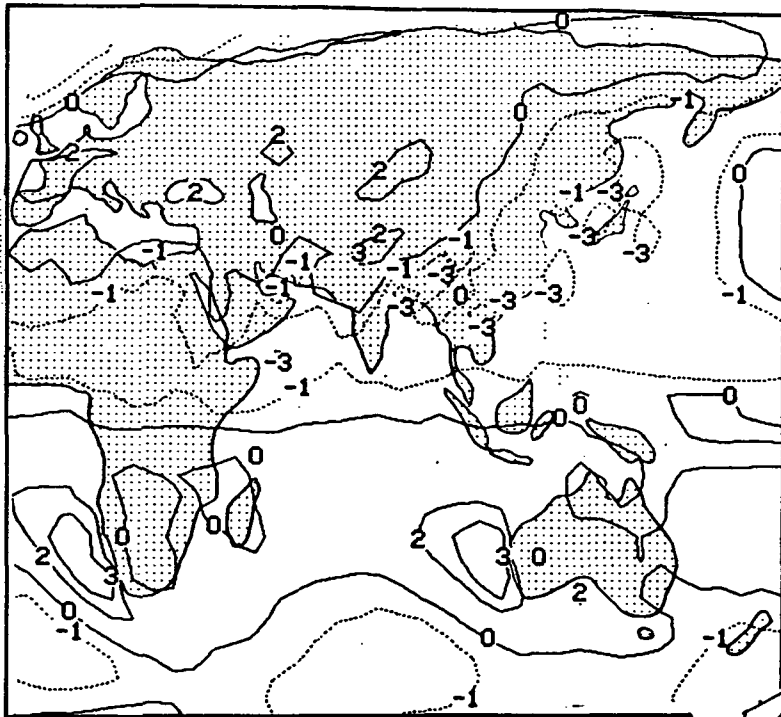


Fig. 10.1 V-component of surface wind (m/s), fine grid Winter (Dec-Jan-Feb)

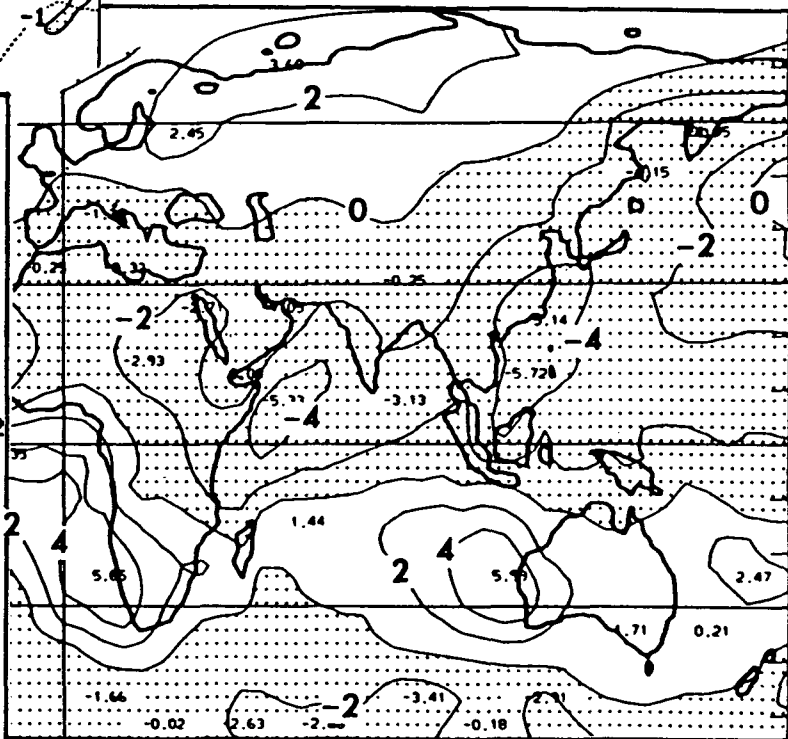


Fig. 10.2 V-component of surface wind (m/s), observed Winter (Dec-Jan-Feb)

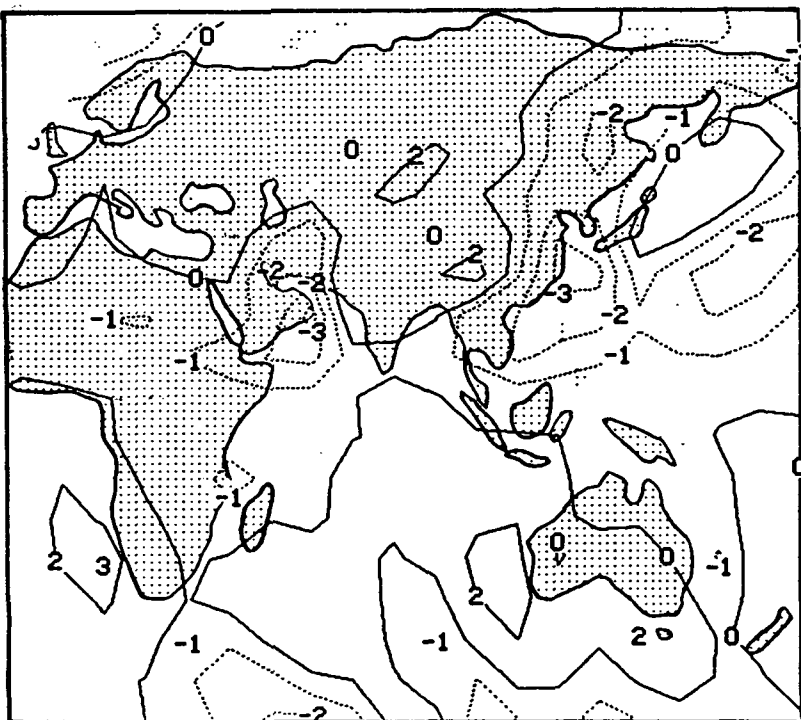


Fig. 10.3 V-component of surface wind (m/s) medium grid, Winter (Dec-Jan-Feb)

11. Cross-equatorial flow, Dec-Jan-Feb

Fine Grid: The seasonal mean V component of the surface wind is verified against the climatological observations of Oort (1983) which are means for 1963-1973.

In the Pacific Ocean, 160°W to South America, the southeasterly trade winds cross the equator giving most V between +1 and +3 m/s. In the model, southerlies do not cross the equator at all, and the average V simulated in this stretch is close to 0.0m/s.

Over equatorial Brazil, observations show the penetration of the northeasterly trade winds giving V between -1 and -2m/s. The model manages $V=-1\text{m/s}$ over northern Brazil, slowing to about -0.5m/s at the equator.

Over the Atlantic Ocean the southeasterly trades should also cross the equator to give positive values of V up to 4m/s. Again, the model shows near-zero cross equatorial flow.

The climatology indicates north to south flow over eastern Africa and the Indian Ocean to the western Pacific. The component V is estimated at about -2m/s along the equator, except for reaching -4m/s in the low-level Somalia jet. In the model, the northerly component of the surface winds is confined to the northern hemisphere, barely reaching -1m/s over Somalia.

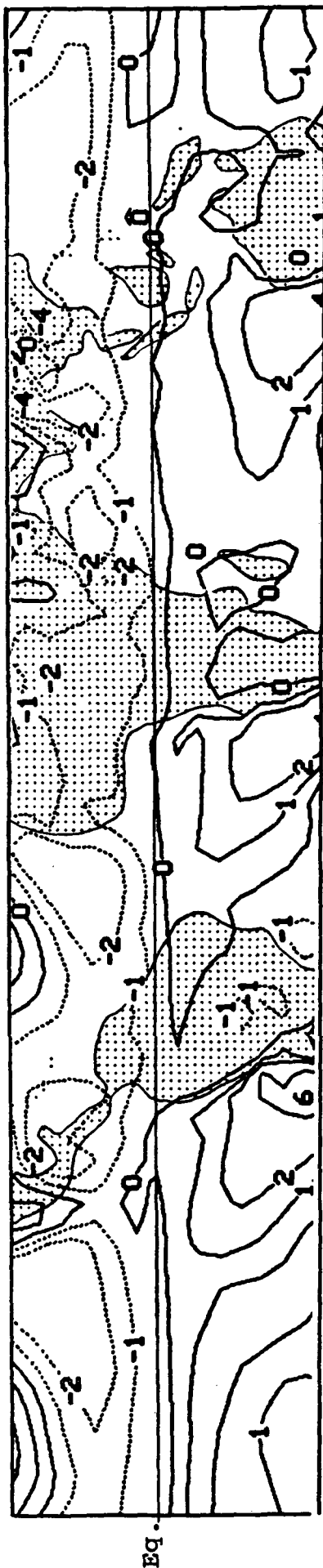
Medium Grid: The model does show northerlies over Brazil and Somalia, and southerlies over the Gulf of Guinea, but much weaker than is observed. Otherwise the cross-equatorial flow simulated by this version during DJF has the same deficiencies as noted above for the fine grid model.

Table 11.1 V-component of surface wind along the equator (m/s), DJF

	<u>Fine Grid</u> (848F9)	<u>Medium Grid</u> (882M9)	<u>Observations</u> (Oort, 1983)
E. Pacific	0.0	+0.5	+1 to +3
S. America	-0.5	-0.5	-1 to -2
E. Atlantic	0.0	+0.5	+2 to +4
E. Africa	-1	-0.5	-2 to -4
Indian Ocean	0.0	0.0	-2 to -4
W. Pacific	0.0	-0.5	-2

Fig. 11.1

V COMPONENT SURFACE WIND (M/S) DJF (FINE GRID) RUN 848 F9



V COMPONENT SURF WIND (M/S)

DJF

(MEDIUM GRID)

882M9

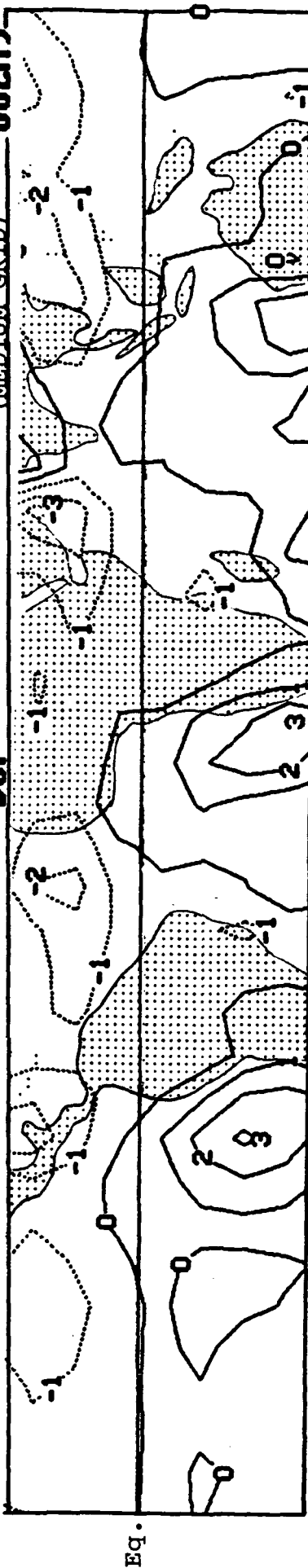
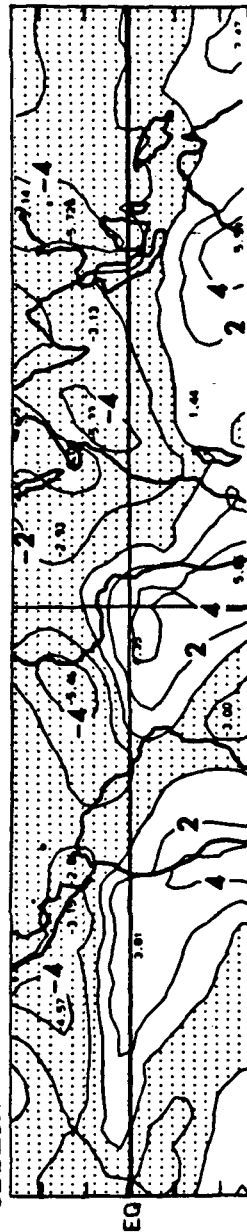


Fig. 11.2

Fig. 11.3 OBSERVED V SFC DJF 63-73



BIBLIOGRAPHIC DATA SHEET

1. Report No. TM 100695	2. Government Accession No.	3. Recipient's Catalog No.	
4. Title and Subtitle Verification of Regional Climates of GISS GCM- Part 1: Winter		5. Report Date January 1988	
		6. Performing Organization Code	
7. Author(s) Leonard M. Druyan and David Rind		8. Performing Organization Report No.	
9. Performing Organization Name and Address Goddard Institute for Space Studies/GSFC 2880 Broadway New York, N. Y. 10025		10. Work Unit No.	
		11. Contract or Grant No.	
12. Sponsoring Agency Name and Address National Aeronautics and Space Adminis.		13. Type of Report and Period Covered Technical Memorandum	
		14. Sponsoring Agency Code	
15. Supplementary Notes Leonard M. Druyan is Senior Research Associate sponsored by the National Research Council of the National Academy of Sciences.			
16. Abstract Verification is made of the synoptic fields, sea-level pressure, precipitation rate, 200mb zonal wind and the surface resultant wind, generated by two versions of the GISS climate model. The models differ regarding the horizontal resolution of the computational grids and the specification of the sea-surface temperatures. Maps of the regional distributions of seasonal means of the model fields are shown alongside maps that show the observed distributions. Comparisons of the model results with observations are discussed and also summarized in tables according to geographic region.			
17. Key Words (Selected by Author(s)) GCM verification model climate verification synoptic climatology simulations		18. Distribution Statement 47/ unclassified/unlimited	
19. Security Classif. (of this report) unclassified	20. Security Classif. (of this page) unclassified	21. No. of Pages 39	22. Price*